SDAC-TR-76-3

12 B.S.

EXPERIMENTAL DETERMINATION OF SCALING LAWS FOR CONTAINED AND CRATERING EXPLOSIONS

ROBERT R. BLANDFORD

Seismic Data Analysis Center

Teledyne Geotech, 314 Montgomery Street, Alexandria, Virginia 22314

4 MAY 1976

Sponsored By

The Defense Advanced Research Projects Agency

Nuclear Monitoring Research Office

1400 Wilson Boulevard, Arlington, Virginia 22209

ARPA Order No. 1620

Monitored By

VELA Seismological Center

312 Montgomery Street, Alexandria, Virginia 22314

Disclaimer: Neither the Defense Advanced Research Projects Agency nor the Air Force Technical Applications Center will be responsible for information contained herein which has been supplied by other organizations or contractors, and this document is subject to later revision as may be necessary. The views and conclusions presented are those of the authors and should not be interpreted as necessarily representing the official policies, either expressed or implied, of the Defense Advanced Research Projects Agency, the Air Force Technical Applications Center, or the US Government.

Unclassified

SECURITY CLASSIFICATION OF THIS PAGE (When Data Entered)

REPORT DOCUMENTATION PAGE

READ INSTRUCTIONS BEFORE COMPLETING FORM

1. REPORT NUMBER: SDAC-TR-76-3
2. GOVT ACCESSION NO.
3. RECIPIENT'S CATALOG NUMBER

4. TITLE (and Subtitle): EXPERIMENTAL DETERMINATION OF SCALING LAWS FOR CONTAINED AND CRATERING EXPLOSIONS.

5. TYPE OF REPORT & PERIOD COVERED: Technical rept.

6. PERFORMING ORG. REPORT NUMBER

7. AUTHOR(s): R. R. Blandford

8. CONTRACT OR GRANT NUMBER(s): F08606-76-C-0004 ARPA Order-2551

9. PERFORMING ORGANIZATION NAME AND ADDRESS
Teledyne Geotech
314 Montgomery Street
Alexandria, Virginia 22314

10. PROGRAM ELEMENT, PROJECT, TASK AREA & WORK UNIT NUMBERS: VT/6709

11. CONTROLLING OFFICE NAME AND ADDRESS
Defense Advanced Research Projects Agency
Nuclear Monitoring Research Office
1400 Wilson Blvd.-Arlington, Virginia 22209

12. REPORT DATE: 04/05/76

13. NUMBER OF PAGES: 77

14. MONITORING AGENCY NAME & ADDRESS (if different from Controlling Office)
VELA Seismological Center
312 Montgomery Street
Alexandria, Virginia 22314

4 May 76

15. SECURITY CLASS. (of this report): Unclassified

15a. DECLASSIFICATION DOWNGRADING SCHEDULE

16. DISTRIBUTION STATEMENT (of this Report)

84p.

APPROVED FOR PUBLIC RELEASE; DISTRIBUTION UNLIMITED.

17. DISTRIBUTION STATEMENT (of the abstract entered in Block 20, if different from Report)

DDC RECEIVED MAR 4 1977 C

18. SUPPLEMENTARY NOTES

19. KEY WORDS (Continue on reverse side if necessary and identify by block number)

Magnitude
Yield
Scaling
Cube-root Scaling
Cratering
Magnitude-Yield
Coupling

20. ABSTRACT (Continue on reverse side if necessary and identify by block number)

Application of cube-root scaling to the observed RAINIER reduced displacement potential for tuff satisfactorily explains spectral ratios over the yield range 0.7 to 1200 kilotons for NTS Pahute Mesa shots detonated below the water table and observed at KNUT and MNNV. The same theory extended to the time domain, assuming a reasonable value for the attenuation parameter of t*=0.1, explains amplitude observations at KNUT and MNNV. However, for no reasonable value of t* can the same reduced displacement

DD FORM 1 JAN 73 1473 EDITION OF 1 NOV 65 IS OBSOLETE

Unclassified

SECURITY CLASSIFICATION OF THIS PAGE (When Data Entered)

408 258

potential explain the observed teleseismic m_b:M_s slope of unity. The only plausible explanation seems to be that the waves emergent vertically downward are significantly different from those emergent vertically upward or nearly horizontally.

As might be expected from Bridgeman's dimensional analysis, no clear empirical scaling conclusions could be derived from our limited data for cratering events. It seems, however, that cratering explosions in the range 20-100 kt generate substantially more Rayleigh waves than do contained explosions in nearly identical media. For body waves there seems to be approximately equal generation of low and high frequency waves, while the cratering explosions seem deficient at intermediate frequencies, 1-3 Hz.

EXPERIMENTAL DETERMINATION OF SCALING LAWS FOR CONTAINED AND CRATERING EXPLOSIONS

SEISMIC DATA ANALYSIS CENTER REPORT NO.: SDAC-TR-76-3

AFTAC Project Authorization No.:	VELA T/6709/B/ETR
Project Title:	Seismic Data Analysis Center
ARPA Order No.:	2551
ARPA Program Code No.:	6F10
Name of Contractor:	TELEDYNE GEOTECH
Contract No.:	F08606-76-C-0004
Date of Contract:	01 July 1975
Amount of Contract:	$2,319,926
Contract Expiration Date:	30 June 1976
Project Manager:	Royal A. Hartenberger (703) 836-3882

P. O. Box 334, Alexandria, Virginia 22314

APPROVED FOR PUBLIC RELEASE; DISTRIBUTION UNLIMITED.

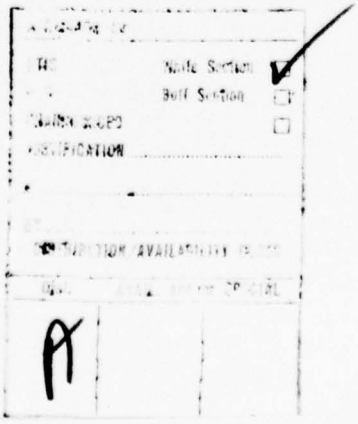

ABSTRACT

Application of cube-root scaling to the observed RAINIER reduced displacement potential for tuff satisfactorily explains spectral ratios over the yield range 0.7 to 1200 kilotons for NTS Pahute Mesa shots detonated below the water table and observed at KNUT and MNNV. The same theory extended to the time domain, assuming a reasonable value for the attenuation parameter of $t^*=0.1$, explains amplitude observations at KNUT and MNNV. However, for no reasonable value of t^* can the same reduced displacement potential explain the observed teleseismic $m_b:M_s$ slope of unity. The only plausible explanation seems to be that the waves emergent vertically downward are significantly different from those emergent vertically upward or nearly horizontally.

As might be expected from Bridgeman's dimensional analysis, no clear empirical scaling conclusions could be derived from our limited data for cratering events. It seems, however, that cratering explosions in the range 20-100 kt generate substantially more Rayleigh waves than do contained explosions in nearly identical media. For body waves there seems to be approximately equal generation of low and high frequency waves, while the cratering explosions seem deficient at intermediate frequencies, 1-3 Hz.

TABLE OF CONTENTS

LIST OF FIGURES

LIST OF FIGURES (Continued)

LIST OF FIGURES (Continued)

LIST OF FIGURES (Continued)

LIST OF TABLES

INTRODUCTION

Many workers in the field of explosion seismology have assumed that cube-root scaling (for which the explosion amplitude in an infinite homogeneous space is proportional to the yield at a time and distance scaled by the cube root of the yield) is valid for contained underground explosions (e.g., Latter et al., 1959; Carpenter et al., 1962; Haskell, 1967; Cherry et al, 1975a,b; Lyuke, Daragan and Peregontseva, 1976). The theoretical foundation for these scaling laws are the dimensional analysis procedures originated by Bridgman (1949). Applications of Bridgman's theory to contained and cratering explosions have been most thoroughly explored by Chabai (1965) who carefully discusses the possible limitations of cube-root scaling.

Latter, A. L., Martinelli, E. A. and E. Teller, 1959, Seismic scaling law for underground explosions, Physics of Fluids, v. 2., p. 280-282.

Carpenter, E. W., R. A. Savill, and J. K. Wright, 1962, The dependence of seismic signal amplitudes on the size of underground explosions, Geophysical Journal, v. 6, p. 426-440.

Haskell, N. A., 1967, Analytic approximation for the elastic radiation from a contained underground explosion, J. Geophys. Res., v. 72, p. 2583-2587.

Cherry, J. T., N. Rimer, J. M. Savino, and W. O. Wray, 1975a, Improved yield determination and event identification research, SSS-R-75-2696, Systems, Science and Software, LaJolla, California.

Cherry, J. T., N. Rimer, and W. O. Wray, 1975b, Seismic coupling from a nuclear explosion: the dependence of the reduced displacement potential on the non-linear behavior of the near-source rock environment, SSS-T-76-2742, Systems, Science and Software, LaJolla, California.

Lyuke, E. I., S. K. Daragan, and V. E. Peregontseva, 1976, Forecasting the Seismic wave spectra of large underground detonations from the spectic of small preliminary explosions, Izvestia, Physics of the Solid Earth, v. 12, p. 103-109.

Bridgman, P. W., 1949, Dimensional Analysis, Yale University Press, New Haven, Connecticut.

Chabai, A. J., 1965, On scaling dimensions of craters produced by buried explosions, J. Geophys. Res., v. 70, p. 5075-5098.

Von Seggern and Blandford (1972) modified Haskell's (1967) parameterization of reduced displacement potential measurements to allow for a discontinuity in the measured velocity at the wavefront, instead of insisting, as did Haskell in his parameterization, that even the acceleration was continuous. This modification, when combined with the ideas of cube-root scaling, led to results in good agreement with observations for the Amchitka explosions LONGSHOT, MILROW, and CANNIKIN.

Cube-root scaling will be valid only so long as the medium is unchanged for all the explosions in the experimental series. At Amchitka the water table is near the surface, well above all the shot points; and the rock type is fairly uniform with depth. There are, presumably, many test sites around the world which fit this description; however, the Nevada Test Site (NTS) is not one of them. The lithology is known to be complicated, and the water table is typically 0.7 km deep, the approximate scale depth of the 65 kiloton (Springer and Kinnaman (1971) explosion DURYEA. Thus because coupling is much better for saturated as compared to unsaturated tuff, one would not be surprised by major changes in the observed explosion source function around 65 kt, the very yield level which is most commonly observed at teleseismic distance. (Smaller events are not detected, larger events are less common.)

Working with NTS data, such workers as Peppin (1974) and Springer and Hannon (1973) have suggested that cube-root scaling is not valid at NTS. This conclusion, on the part of the first study in which the data was analyzed in the spectral domain, may be criticized on the basis that the author did not ensure that the medium was consistent for all yields. Springer and Hannon (1973) did control the medium, but performed their analysis in the time domain. We shall show in this report that interacting effects of cube-root scaling,

---

von Seggern, D. and R. Blandford, 1972, Source time functions and spectra for underground nuclear explosions, Geophys. J. R. Astr. Soc., v. 31, p. 83-97.

Peppin, W. A., 1974, Discrimination among small magnitude events on Nevada Test Site, Geophys. J. R. Astr. Soc., v. 37, p. 227-243.

Springer, D. and W. Hannon, 1973, Amplitude-yield scaling for underground nuclear explosions, Bull. Seism. Soc. Amer., v. 63, p. 477-500.

Springer, D. L. and R. L. Kinnaman, 1971, Seismic source summary for U.S. underground nuclear explosions, 1961-1970, v. 61, p. 1073-1098.

depth of burial, attenuation, and instrument response can conceal the effects of cube-root scaling in the time domain by "straightening out" a magnitude-yield curve. A hint of this effect may be found in the fact that Springer and Hannon found different magnitude-yield slopes for regional and teleseismic stations. We shall see that this can be partially explained by the strong effects of absorption on measurements in the time domain. The remaining effect, we shall suggest, is due to differing waveforms emitted vertically downward and horizontally.

Since the question of the proper scaling of explosions in a given medium is of profound importance, both with respect to discrimination in a comprehensive test-ban treaty, and with respect to magnitude-yield relations in a threshold test-ban treaty, we will try in this report to unequivocally establish that cube-root scaling with discontinuous wavefront velocity is the proper scaling law for explosions in a fixed medium. We do this by using data from MNNV and KNUT, only 2-3° from the test site; and by using yields which range over 3.2 orders of magnitude.

DATA AND TECHNIQUE

Table I is a list of the NTS events considered in this study, and Figure 1 is a map of the NTS area from Springer and Hannon (1973) on which may be found all of the events in Table I except events SEDAN and PAR. These latter two events are located about 30 km to the east within about 5 km of one another.

In Figure 2 we see the vertical, radial, and transverse components at KNUT and MNNV of the four events detonated below the water table (Table I). The first arrival is P_n, the second arrival P_g. All short-period data are sampled at 40 samples per second. We see that the signal-to-noise ratio is good, and that P_g arrives approximately 7 seconds into the signal at KNUT and 2 seconds at MNNV. In the case of REX, this arrival clipped even the low-gain analogue tape channel, so that only data up to this point may be analyzed. Examination of the data for other events shows that the BENHAM data is unclipped only up to 9 seconds at KNUT and only up to 4 seconds at MNNV. For DURYEA the corresponding times are 7 seconds and 2.5 seconds. The short-period data for all other events considered are valid up to at least 10 seconds, the maximum length data sample used in this study.

Since only spectral ratios of one event to another were of interest, the analysis procedure is to average the logarithms of the spectral ratios for every component possible. As an example, consider the REX/BUTEO ratio. For KNUT the spectrum of the first 7 seconds of Z, R, and T for the REX signal are divided by the spectrum of the first 7 seconds for BUTEO. This yields three ratios. Three more ratios are determined by the first 2 seconds of MNNV signal data. The logarithms of all 6 spectral ratios are then averaged to give the final result.

It might be objected that inclusion of the radial and transverse component ratios will lead to a large amount of "strain release" energy being included in the ratios. However, since the emergence angle is approximately 45° at distances of 2-3°, there would be as much strain energy in the vertical component as in the radial component. For the following theoretical reasons, we believe that there is little strain energy in the spectra.

TABLE I

Event Parameters

Event Date	Origin Time	Yield (kt)	Depth (ft) (km)	Elevation (ft)	Latitude Longitude	Medium Moisture Content (wt %)	Static Water Table Depth (ft) Paleozoic Layer Depth (ft)
BUTEO 12 May 65	19 15 00.10	L (0.7 est)	2282 0.69	6520	37 14 33.6N 116 25 51.1W	Tuff	2170 >20000
			(τ = .74) [.9] ⟨.71⟩				
REX 24 Feb 66	15 55 07.4	16 (19 est)	2204 0.67	6557	37 16 18.6N 116 26 01.8W	Tuff	2105 (m)
			(τ = .72) [.89] ⟨.81⟩				
DURYEA 14 Apr 66	14 13 43.10	65	1786 0.54	6520	37 14 33.6N 116 25 51.1W	Rhyolite	2170 >20000
			(τ = .60) [.65] ⟨.80⟩				
SCOTCH 23 May 67	14 00 00.04	150	3207 0.98	6761	37 16 30.3N 116 22 11.9W	Tuff 17	2210 >20000
			(τ = .92) [1.02] ⟨.85⟩				
BENHAM 19 Dec 68	16 30 00.04	1100	4600 1.41	6281	37 13 53.3N 116 28 24.9W	Tuff	2105(m) >20000
			(τ = 1.21) [1.2] ⟨1.12⟩				

( ) τ values from Cohen et al. (1972) SDL 282 Figure 36
[ ] values from Frasier (1972) Geoph. J. R. Astr. Soc., 35, p. 99-109, Figure 5.
⟨ ⟩ this report

TABLE I (Continued)

Event Parameters

Cratering Explosions

PALANQUIN 14 Apr 65	13:14:00.11	4.3	280 .085	6194	37 16 49.4N 116 31 24.8W	Rhyolite	2194 >20000
CABRIOLET 26 Jan 68	16:00:00.11	2.3	170 .052	6197	37 16 51.1N 116 30 52.0W	Rhyolite	2000
SCHOONER 08 Dec 68	16:00:00.14	35	350 .107	5563	37 20 36.3N 116 33 57.1W	Tuff	900 >10000
SEDAN 06 Jul 62	17:00:00.14	100	635 .193	4317	37 10 37.2N 116 02 43.4W	Alluvium 9% water	1890 1300
PAR 09 Oct 64	14:00:00.12	38	1325 .40	4368	37 09 04.8N 116 04 37.2W	Alluvium 14% water	1950 2650

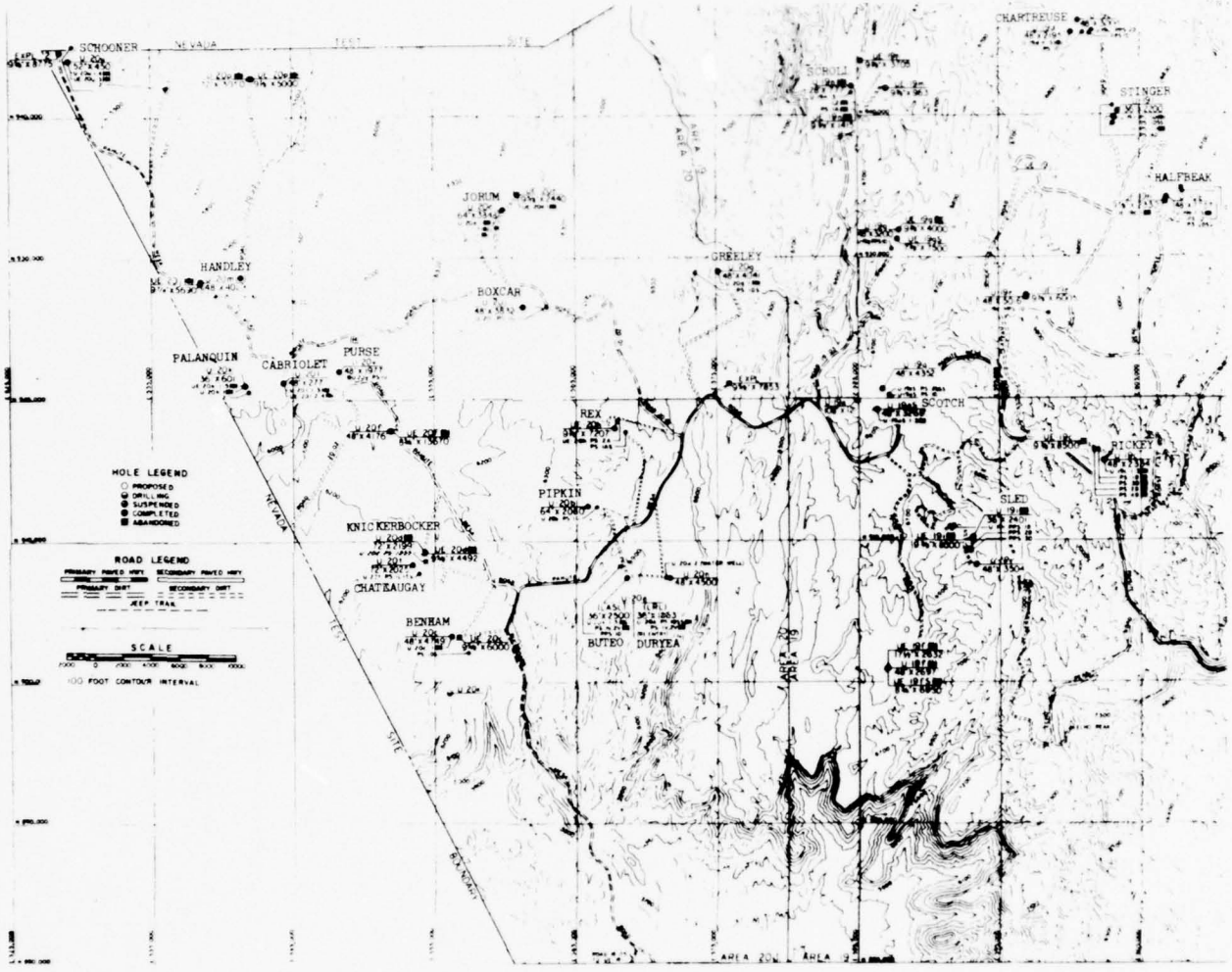

Figure 1. Map of Pahute Mesa, from Springer and Hannon (1973).

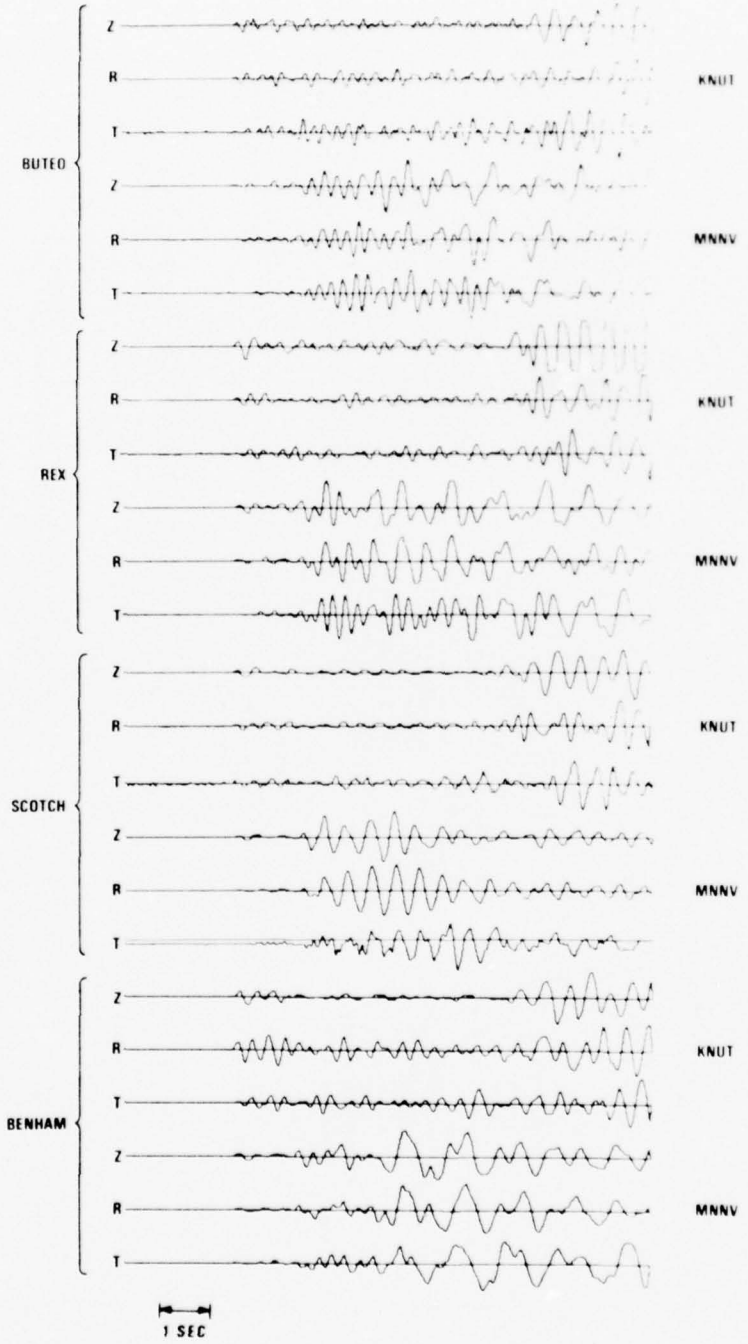

Figure 2. Three components of short-period motion at KNUT and MNNV, for BUTEO, REX, SCOTCH, and BENHAM.

Toksöz and Kehrer (1972) have generally found that the long-period (20 sec) strain release Rayleigh amplitudes to be less than those created directly from the explosion compressional waves. Most of the strain release Rayleigh waves come from shear waves, but the compressional to shear ratio for earthquakes is approximately 1:6 (Blandford, 1975). Thus as long periods we typically expect the direct strain release P waves to be less than 1/6 that from the explosion. But theory also suggests that the long-period to short-period ratio for earthquakes is greater than for explosions (Blandford, 1975). Finally, there is still a question in the minds of some workers (Blandford and Clark, 1974) as to whether the evidence for the existence of strain release is satisfactory. Near-source propagation and source asymmetries due to instabilities may also be invoked to account for the existence of Love waves emerging from the explosion epicenter.

From an experimental point of view one may justify the averaging of all three component ratios by the observation that in every case each of the three show the same overall trends; the only effect of the averaging is to reduce scatter. Also, the time domain amplitude ratio between components was constant from event to event over the magnitude range 0.7 to 1200 kilotons, this would not be expected if variable and significant proportions of strain release were involved.

Each individual spectrum is calculated as follows. The first point of the time series is selected to be 2.5 seconds in front of the signal. The noise-plus-signal window is detrended, and a 2.5 second cosine taper is applied to the start of the data thus giving a smooth "lead-in" to the signal. The end of the signal is tapered with a 1.0 second cosine taper. The resulting

---

Toksöz, M. N. and H. H. Kehrer, 1972, Tectonic strain release by underground nuclear explosions and its effect on seismic discrimination, Geophys. J. R. Astr. Soc., v. 31, p. 141-161.

Blandford, R., 1975, A source theory for complex earthquakes, Bull. Seism. Soc. Am., v. 65, p. 1385-1406.

Blandford, R. and D. Clark, 1974, Detection of long-period S from earthquakes and explosions at LASA and LRSM stations with application to positive and negative discrimination of earthquakes and underground explosions, SDAC-TR-74-15, Teledyne Geotech, Alexandria, Virginia. ADA 013 672

tapered waveform is supplemented with sufficient zeros to fill out a 512-point array, and the amplitude spectrum is calculated using the Fast Fourier Transform.

Since the underground explosions are within 10 km of each other, the time interval between P_n and P_g is the same for practical purposes for each event. Thus each event has a nearly identical proportion of each phase. Thus even if there are different transfer functions for each phase, e.g. H_1 and H_2, they will cancel out of the spectral ratio. For two events, a and b, the Fourier transforms of phase 1 and phase 2 together are $(S_a H_1 + S_a H_2)$ and $(S_b H_1 + S_b H_2)$. Factoring out $(H_1 + H_2)$ the amplitude spectral ratio is $|S_a|/|S_b|$ where S_a and S_b are the Fourier amplitude spectra of events a and b.

SCALING RESULTS IN THE SPECTRAL DOMAIN FOR BURIED EXPLOSIONS

Examination of Figure 1 and of the data in Table 1 shows that the greatest distance between any two of the first 5 events is 10 km between BENHAM and SCOTCH. Furthermore, all of these events, except DURYEA, are below the water table. BUTEO and REX are much deeper than normal for their yield, thus they are in a common medium making the yield sequence BUTEO, REX, SCOTCH, BENHAM uniquely valuable for a study of amplitude-yield relations at NTS.

In Figure 3 we see the data for each of the first five contained explosions in Table 1 up to just before the point at which the REX data clipped. At KNUT it is apparent to the eye that BUTEO has substantially higher frequency energy than does BENHAM, suggesting that BUTEO's displacement amplitude spectrum begins to fall off at a higher frequency.

In Figure 4 we see the amplitude spectrum of the KNUT data displayed in Figure 3. Here we can see explicitly that the "corner frequency" for BUTEO is much higher than for BENHAM.

In order to apply scaling theory to these data it is essential to have accurate estimates of the yields. Almost all authors are in agreement that M_s:yield relationships are linear with a slope of 1.0. We shall assume that this is the case and use von Seggern's (1973) M_s estimates to establish a corrected yield for REX and, together with LR measurements at MNNV for BUTEO and REX, a yield estimate for BUTEO.

Fitting a line of slope unity to the M_s:yield points of SCOTCH and BENHAM, and using von Seggern's M_s estimate gives an estimated yield for REX of 19 kt.

In Figure 5 we see tracings of the MNNV long-period data for BUTEO, REX and BENHAM. It is quite clear that the system is responding non-linearly for BENHAM. Note also that the signal shape is significantly different for BUTEO and REX. (The only available LR signal for BUTEO is at MNNV, the long-period vertical instrument was inoperative at KNUT for BUTEO.) Examination

---

von Seggern, D. H., 1973, Joint magnitude determination and analysis of variance for explosion magnitude estimates, Bull. Seis. Soc. Am., v. 63, #3, p. 827-845.

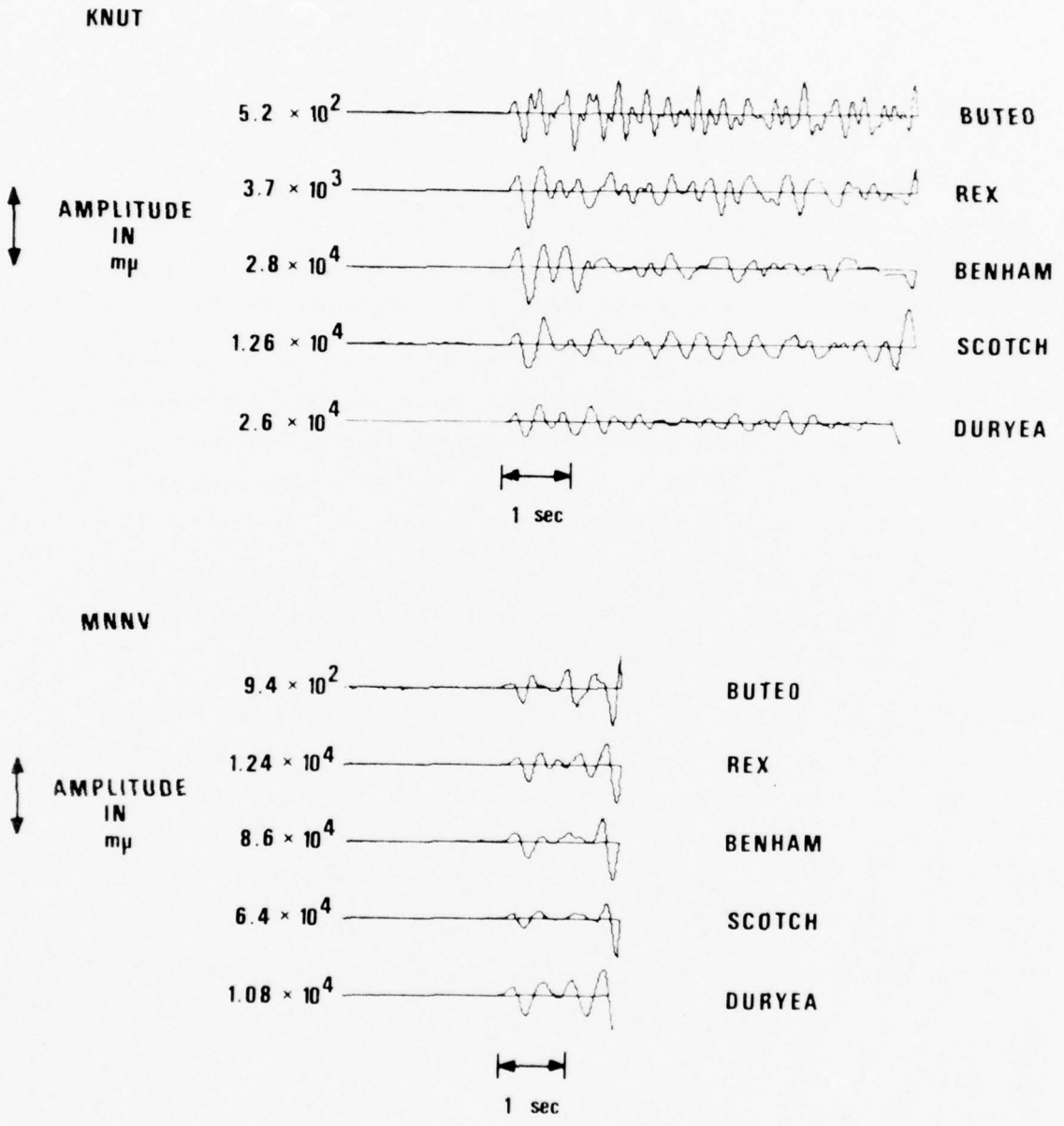

Figure 3. First few seconds of short-period motion at KNUT and MNNV for BUTEO, REX, BENHAM, SCOTCH, and DURYEA.

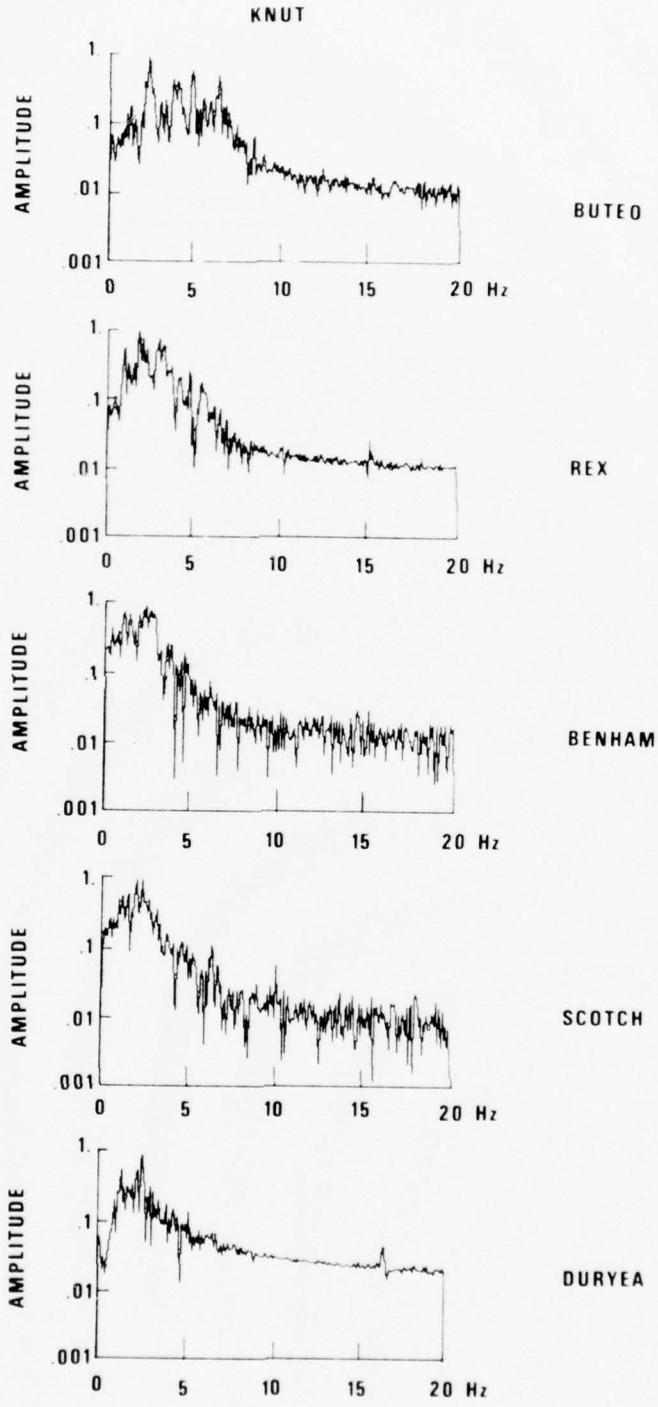

Figure 4. Log-amplitude spectra at KNUT for the time windows shown in Figure 3 for BUTEO, REX, BENHAM, SCOTCH, and DURYEA.

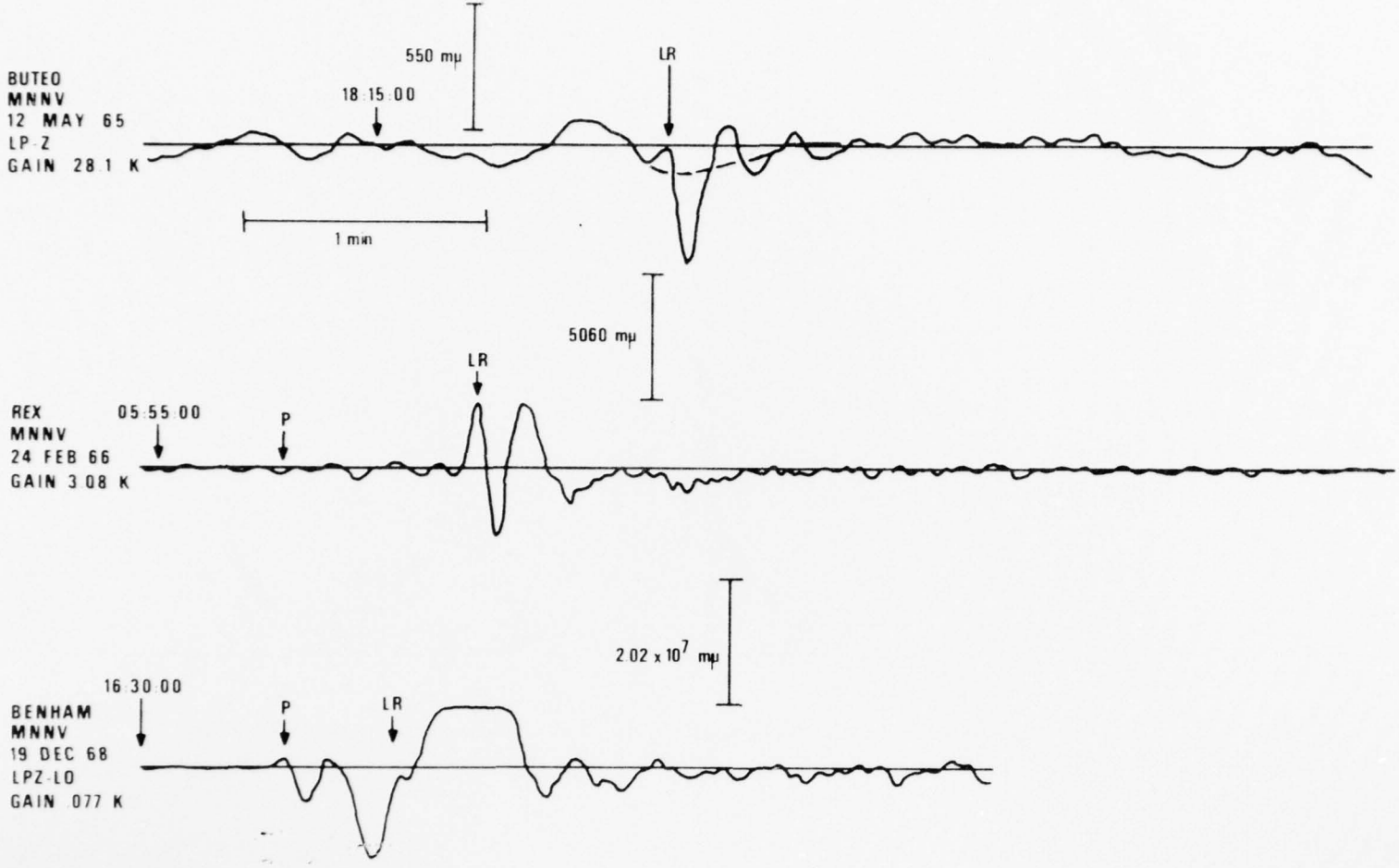

Figure 5. Long-period waveforms recorded at MNNV for BUTEO, REX, and BENHAM. Both the REX and BENHAM records show non-linear distortion.

of the Basin and Range fundamental mode dispersion diagrams in Glover and Alexander (1970) shows that there is a maximum in the group velocity between 10 and 12 seconds, the period of the initial LR pulse in BUTEO and REX. The typical relative delay at this distance for periods of 4 to 6 seconds would be 10 seconds. Thus we would not be surprised to find that the arrival of signal with these periods shortly following the first pulse of the LR signal had driven the system into non-linearity. For this reason we have chosen to determine the relative yield of BUTEO and REX by comparing the corresponding amplitudes of the first LR pulse. In Figure 5 we see the subjectively drawn baseline for the BUTEO signal. Measuring from this baseline the result is an estimated yield of 0.7 kt for BUTEO.

To predict theoretical short-period spectral ratios for comparison with observation we therefore use for REX and BUTEO the yields of Table 1 which are indicated as "estimated". These yield values are inserted in the theoretical source spectrum of von Seggern and Blandford (1972) using the source spectrum parameter values B=0, k_o=12 determined by fitting the Rainier tuff data presented by Haskell (1967). The formulas for the von Seggern-Blandford amplitude spectrum $S(\omega)$ are:

$$S(\omega) = Y \frac{[A^2(\omega/k)^2 + 1]^{1/2}}{[(\omega//k)^2 + 1]^{3/2}}$$

$$A = 1 + 2B; \; k = k_o(5/Y)^{1/3} \qquad (1)$$

To model the effects of the surface reflection on the amplitude spectrum we multiply by

$$[1 + \alpha^2 - 2\alpha \cos\omega\tau]^{1/2} \qquad (2)$$

which is the amplitude spectrum of two delta functions of opposite sign and relative amplitude α separated by time τ. In Table I estimates for τ are

---

Glover, P. and S. S. Alexander, 1970, A comparison of the Lake Superior and Nevada Test Site source regions, Seismic Data Laboratory Report 243, Teledyne Geotech, Alexandria, Virginia. AD 865 512.

given which were calculated using data in the papers of Cohen et al (1972) and Frasier (1972). We also give τ values obtained in the present study by attempts, described below, to fit the observed spectral ratios.

In Figures 6a-c we see the observed spectral ratios of REX, SCOTCH, and BENHAM, to BUTEO. Superimposed on these figures are the theoretical spectral ratios appropriate to the yields, with and without the effects due to pP. The irregularity of the theoretical ratio in Figure 6c arises from the interplay of the BUTEO and BENHAM nulls which occur at different frequency intervals. We have determined reflection coefficients of 0.7 for BUTEO and 0.5 for the others. The τ values listed in Table 1 are those determined by inspection to give the best fit to the data. We should note at this point that for REX the non-linear zone, on the order of 100 meters radius, would extend above the water table. However, we may still expect near-saturation within 200 feet of the water table.

We see that in general the ratios without pP factors give a satisfactory fit overall. However, there seems little doubt that many of the details especially for $0.5 < f < 2.0$ Hz are influenced by pP.

It is noticeable that all of the ratios seem to be less than the theoretical ratio for $f < 0.5$ Hz. Spectra of the noise in front of all the channels were computed and it was found that for BUTEO $(S/N) \bar{<} 1.0$ on all channels for $f < 0.5$ Hz. This presumably reflects the fact that the microseisms are of appreciable size in comparison to an explosion of this small a yield and explains the lower than expected ratios in this frequency range. For the events BUTEO, DURYEA and SCOTCH, $(S/N) \bar{<} 1$ on some of the channels over some portions of the frequency range $5 < f < 8$ Hz. Examination of the other ratios, e.g. BENHAM/SCOTCH, seems to show $(S/N) \bar{<} 1$ for $f < .4$ Hz for REX, SCOTCH, and DURYEA.

Cohen, T. J., R. L. Sax, and H. L. Husted, 1972, Spectral whitening with application to explosion pP, Seismic Data Laboratory Report 282, Teledyne Geotech, Alexandria, Virginia. AD 750 781.

Frasier, C. W., 1972, Observations of pP in the short-period phases of NTS explosions recorded at Norway, Geophys. J. R. Astr. Soc., v. 31, p. 99-109.

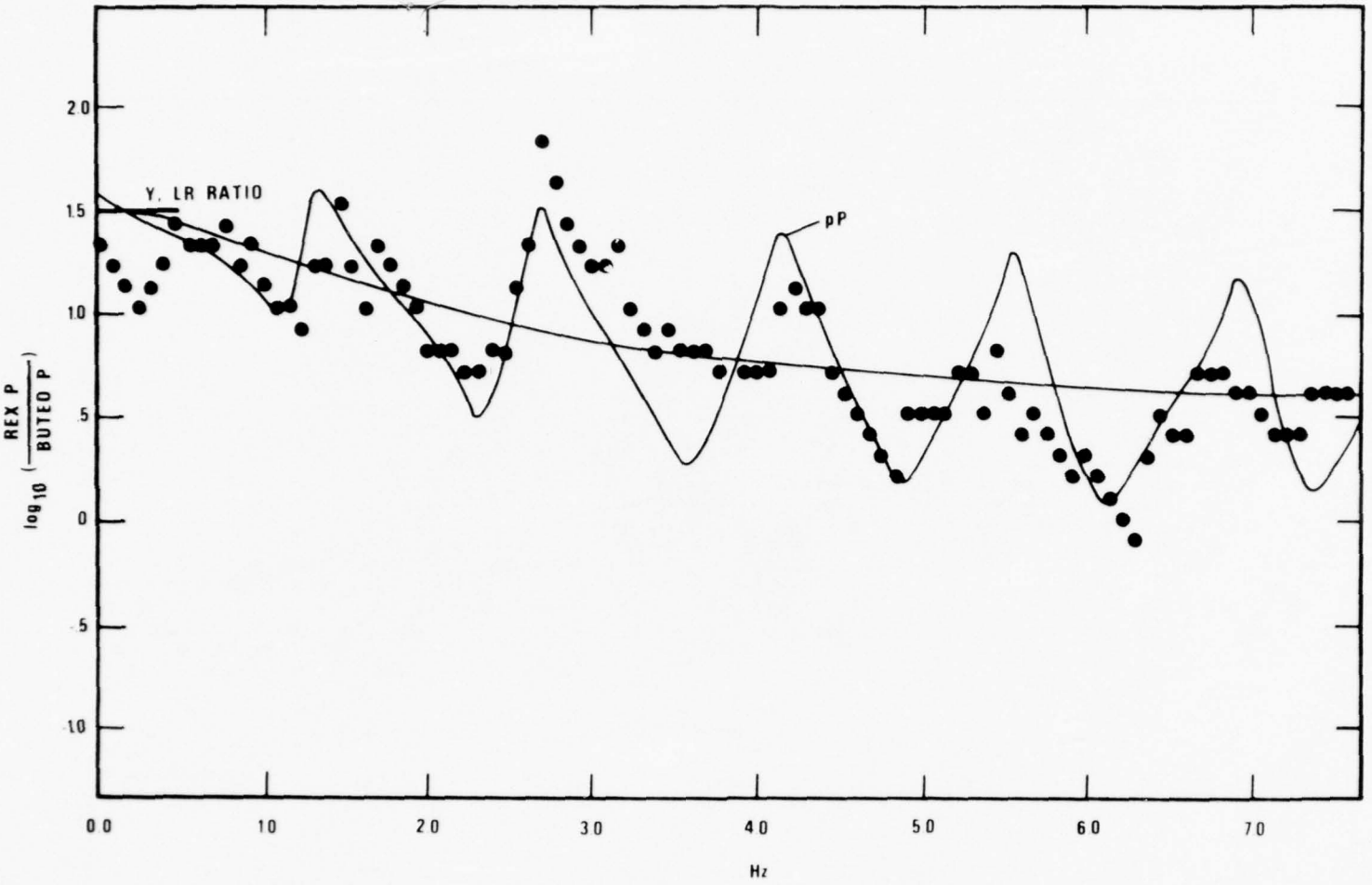

Figure 6a. Dots give the observed spectral ratio REX/BUTEO. The theoretical spectral ratios appropriate to the tuff model, B=0, k_O=12 have been superimposed, with and without the effect of pP included.

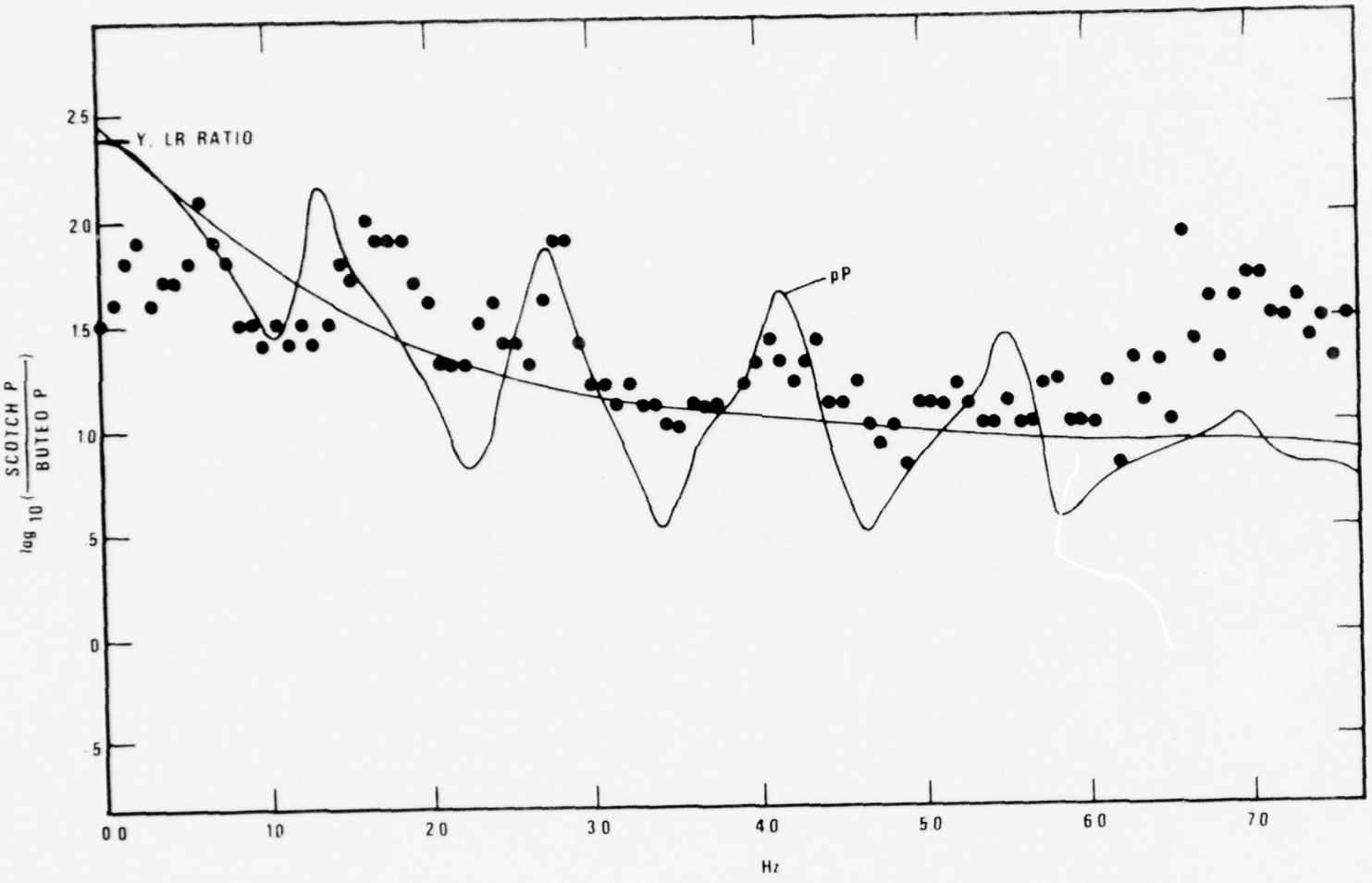

Figure 6b. Dots give the observed spectral ratio SCOTCH/BUTEO. The theoretical spectral ratios appropriate to the tuff model, B=0, k_o=12 have been superimposed, with and without the effects of pP included.

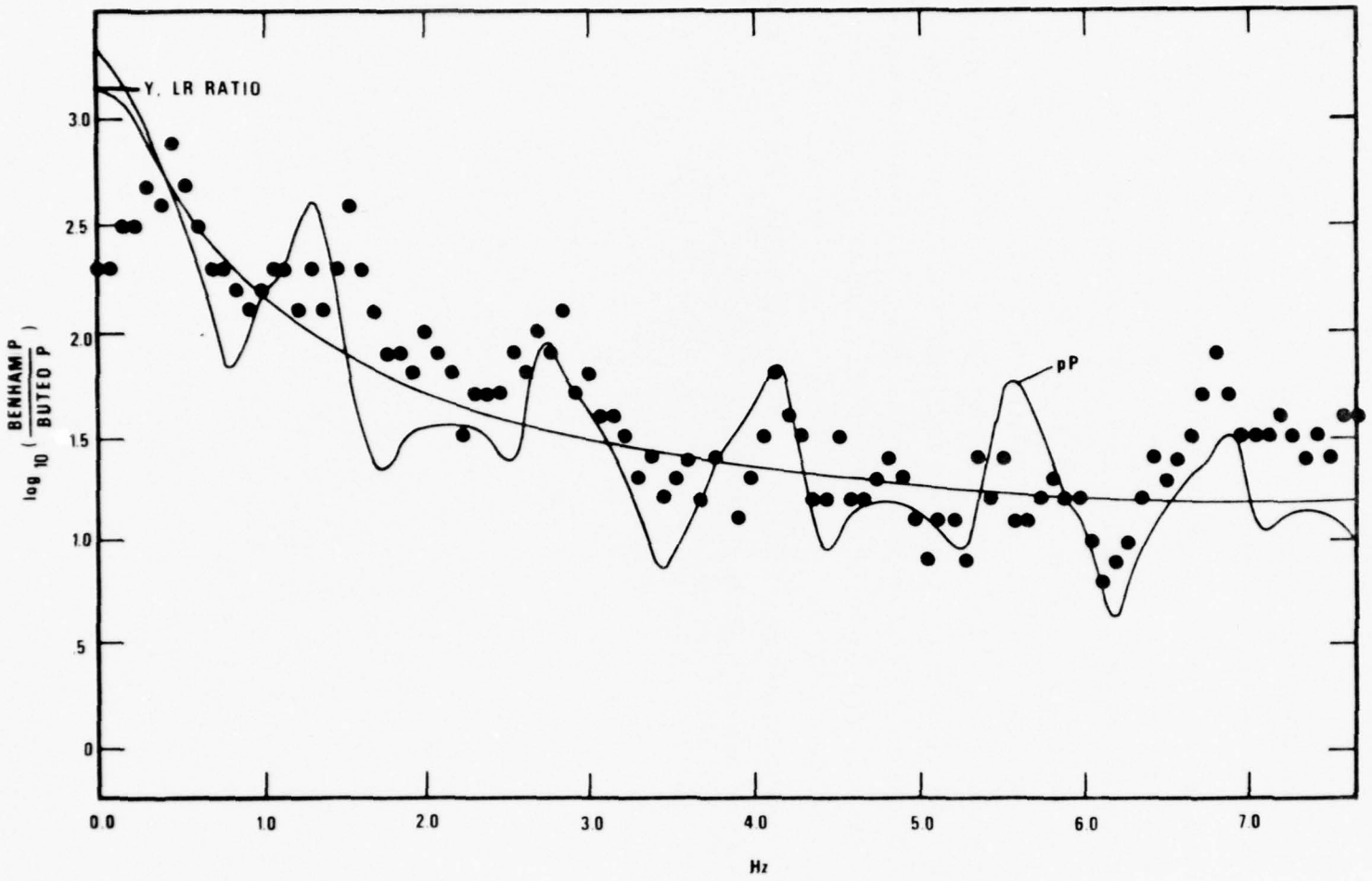

Figure 6c. Dots give the observed spectral ratio BENHAM/BUTEO. The theoretical spectral ratios appropriate to the tuff model, B=0 k_o=12 have been superimposed, with and without the effects of pP included.

The low-frequency theoretical ratios without the effects of pP included do tend asymptotically to the observed LR-amplitude ratios. Of course, in the case of REX/BUTEO they must do so since the estimated relative yields in this case were determined directly from these relative amplitudes.

In the cases of SCOTCH/BUTEO and BENHAM/BUTEO, the asymptotic limits must also agree closely with observation since the REX, and hence the BUTEO, yield was determined by a fit to the SCOTCH and BENHAM yields.

It would seem to be impossible to view Figure 6c, in which the BENHAM/BUTEO theoretical spectral ratio ranges over 2.0 magnitude units and is in good agreement with observations (except for $f < 0.5$ Hz where noise in the BUTEO data is an explanation), and not believe that there is indeed a very powerful scaling effect of spectrum with yield. It seems perfectly clear from the data that there is a substantial change of corner frequency with yield. If we choose the corner frequency as the point where $(\omega/k) = 1.0$ in the theoretical source spectrum (1/2 amplitude point), for Y=0.7 kt it is located at 3.7 Hz, and for Y=1100 kt, at 0.31 Hz.

SCALING RESULTS IN TIME DOMAIN FOR BURIED EXPLOSIONS

To compare predictions with observations in the time domain, it is necessary to compute actual waveforms. To do this we compute the wavelet spectrum as the product of the source spectrum, (equation (1)), an amplitude attenuation operator $e^{-\omega T/2Q} = e^{-\omega t^*/2}$ where T is the travel-time and Q is the quality factor, and the LRSM short-period instrument response. The Hilbert transform of the log-spectrum is then calculated to determine the minimum phase corresponding to the spectrum. Instead of using the Hilbert transform, it would be possible to use Futterman's phase for attenuation (Werth et al., 1962), the measured LRSM phase response, and the wavelet corresponding to the source spectrum. The present procedure gives the same result and seems simpler and more flexible. The complex phase is multiplied by the amplitude spectrum, and when the full spectrum is inverted into the time domain there results the minimum-phase wavelet. This wavelet is then convolved with delta functions having the appropriate polarities, amplitudes and time delays to give P and pP.

The time interval between P and pP used in this paper for waveform time domain calculations is $\tau = .12Y^{1/3}$ (with Y in kilotons) which was used by Douglas et al. (1972) for granite; and which may be derived from the USSR containment depth formula $h = .16Y^{1/3}$ km together with a velocity for Kazakh of 2.75 km/sec; Marshall (1972). A similar formula may be derived for NTS tuff events by plotting the yield of events of known yield in tuff versus depth, and assuming a velocity of known yield in tuff versus depth, and assuming a velocity of 2.5 km/sec; see for example Marshall (1972). This yields $\tau = .15Y^{1/3}$ sec. In this study we assume for all events, $\tau = .12Y^{1/3}$ since for most purposes the difference between the formulas is negligible. Specific cases of interest in the future could be investigated individually.

Werth, G. C., R. F. Herbst, and D. L. Springer, 1962, Amplitudes of seismic arrivals from the M discontinuity, J. Geophys. Res., v. 67, p. 1587-1610.

Marshall, P. D., A. Douglas, and J. Hudson, 1971, Surface waves from underground explosions, Nature, v. 234, p. 8-9.

In Figure 7a we have plotted the calculated amplitude (in arbitrary units) of the P-wave first motion versus yield for explosions in tuff. We see that the slope changes from a value close to 1.0 for yields less than 1 kt, to a slope close to 0.5 around 100 kt. Since the amplitude beyond the corner frequency in the von Seggern-Blandford ω^{-2} model increases as the cube-root of the yield, the asymptotic slope for large yields must be 0.33.

Note that the effect of increasing values of t* is to increase the slope, while of course reducing the absolute amplitude. Carpenter (1966) and Douglas et al. (1973) used a value of T/Q = t* = 1.0 for prediction of teleseismic records. Trembly and Berg (1968) used t* = 1.0 for the path NTS-NPNT. Frasier and Filson (1972), Frasier (1972), and Noponen (1975) calculated values between 0.4-0.5 for the NTS-NORSAR path. Der and McElfresh (1975) deduced values of about 0.1 from Louisiana to the Eastern United States, and of about 0.5 to the Western United States. For their results to be consistent with 0.4-0.5 for NTS-NORSAR they required a Q of 3000 in the lower mantle. Noponen (1975) also deduced a value for t* of 0.2 for the Kazakh-NORSAR path.

Detailed investigation by the author of the supporting studies for t* > 0.5 reveals generally unconvincing partial or preliminary analyses. Thus in this study we concentrate on values for t* of less than 0.6.

Carpenter, E. W., 1966, A quantitative evaluation of teleseismic explosion records, Proc. Roy. Soc., A., v. 290, p. 396-407.

Douglas, A., J. A. Hudson, and C. Blamey, 1972, A quantative evaluation of seismic signals at teleseismic distances---III computed P and Rayleigh wave seismograms, Geo. J. R. Astr. Soc., v. 28, p. 385-410.

Trembly, L. D. and J. W. Berg, 1968, Seismic source characteristics from explosion-generated P waves, Bull. Seism. Soc. Am. v. 58, p. 1833-1848.

Frasier, C. W. and J. R. Filson, 1972, A direct measurement of the earth's short-period attenuation along a teleseismic ray path, J. Geophys. Res., v. 77, p. 3782-2787.

Noponen, I., 1975, Compressional wave power spectrum from seismic sources, Institute of Seismology, University of Helsinki, ISBN 951-45-0538-7. Contract AFOSR-72-2377 Final Report.

Der, Z. A. and T. W. McElfresh, 1975, Short-period P-wave attenuation along various paths in North America as determined from P-wave spectra of the SALMON nuclear explosion, SDAC-TR-75-16, Teledyne Geotech, Alexandria, Virginia.

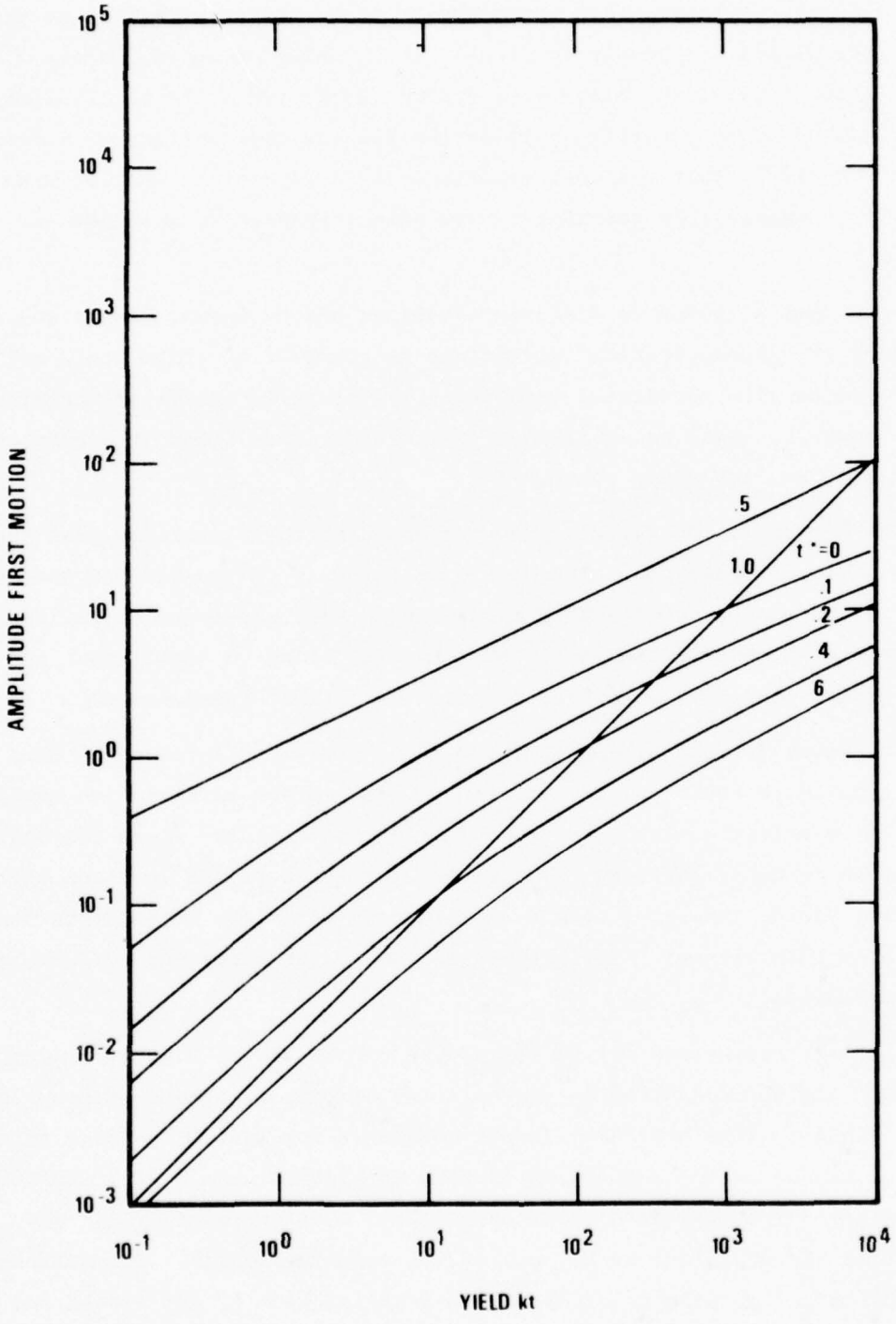

Figure 7a. Theoretical amplitude-yield curve for t*=0, 0.1, 0.2, 0.4, 0.6; tuff, amplitude of first motion, no surface reflection.

In Figure 7a we see that the m_b vs. Y slope varies with t*. At megaton yields the slopes are nearly identical with a value of approximately 0.43 while at 10 kt yield the slope varies from .68 to .91 as t* varies from 0 to 0.6. This could be a partial explanation for the observations of Springer and Hannon (1973) that regional magnitude-yield slopes are smaller than teleseismic ones. This possibility was also suggested by Springer and Hannon.

Note that if paths to different stations had different slopes due to different t* values, station corrections independent of yield would not be sufficient to give consistent magnitudes. Internally consistent magnitudes could, however, still be obtained if measurements are taken at a complete set of stations for every event.

For Figure 7a the calculations proceeded on the assumption that there was no surface reflection. This would be valid if the upward coupling were weak, if the surface were highly irregular so that non-specular reflection occurred, or if significant spall occurred resulting in significant non-linear energy transfer to frequencies not detectible teleseismicly.

In Figure 7b we assume that there is a surface reflection and that the reflection is perfect. Since this figure also is for first-motion amplitude, there is no effect on the results except for small yields where the containment depth is quite shallow. Comparison of Figures 7a and 7b shows that for small yields the first motion amplitude is much less with the surface reflection than without. (Note that this would not apply for BUTEO which was over-buried.)

Similar conclusions may be reached by comparison of Figures 7c and 7d where the amplitude plotted is one-half the maximum trough-to-peak amplitude of the signal. (The amplitude is not corrected for system response at the apparent period of the motion, as is done in Figures 7e and 7f.) In this case we may see by detailed comparisons that at intermediate yields pP reinforces the amplitude by as much as 0.2 magnitude units. The maximum enhancement may be seen to occur around 2 kt for t* = 0, and around 200 kt for t* = 0.6. At large yields the amplitudes are identical to 7c and 7d because the direct and reflected pulses are separated in time and are of equal amplitude.

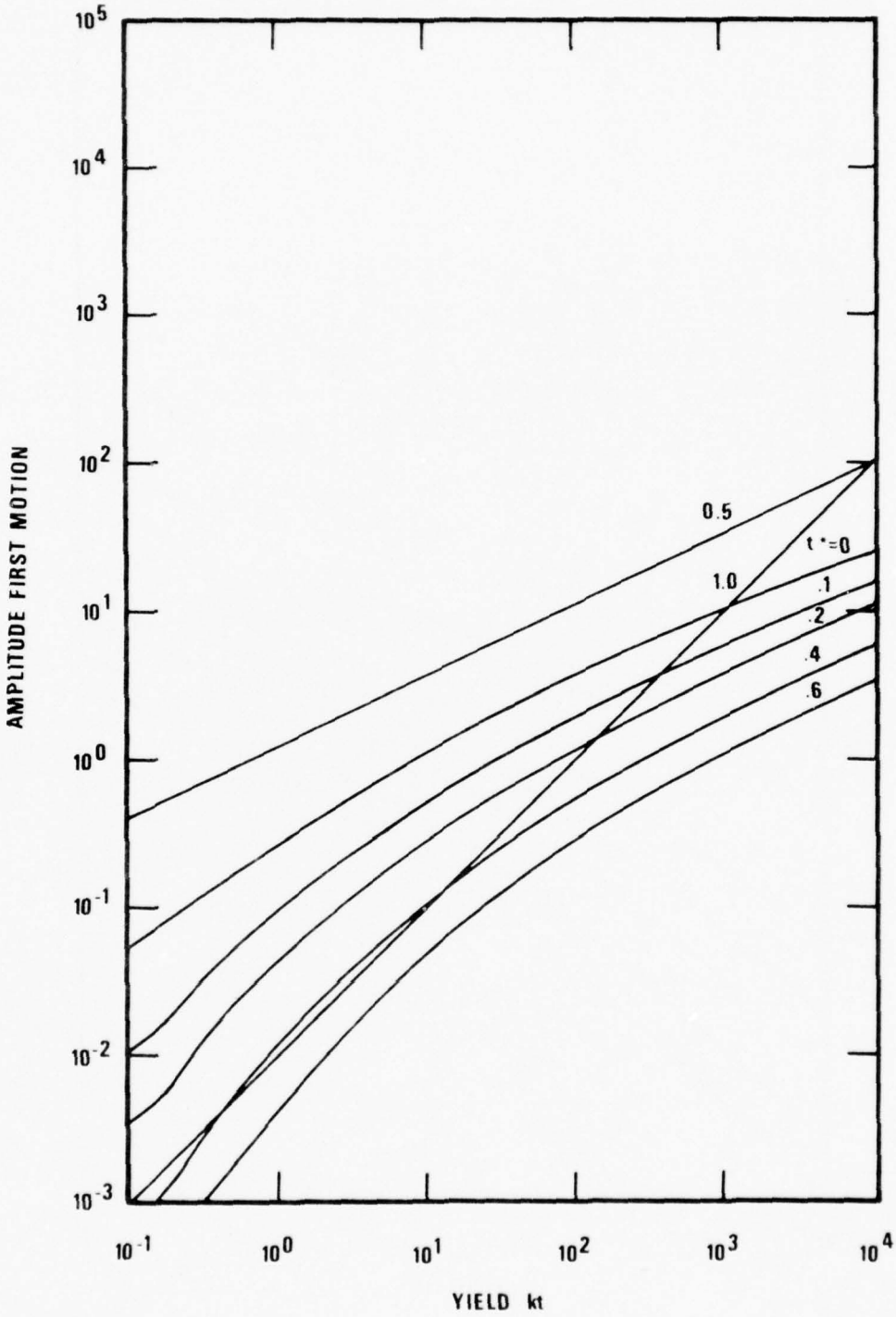

Figure 7b. Theoretical amplitude-yield curve for t*-0, 0.1, 0.2, 0.4, 0.6; tuff, one-half maximum peak-to-peak amplitude of signal, no surface reflection.

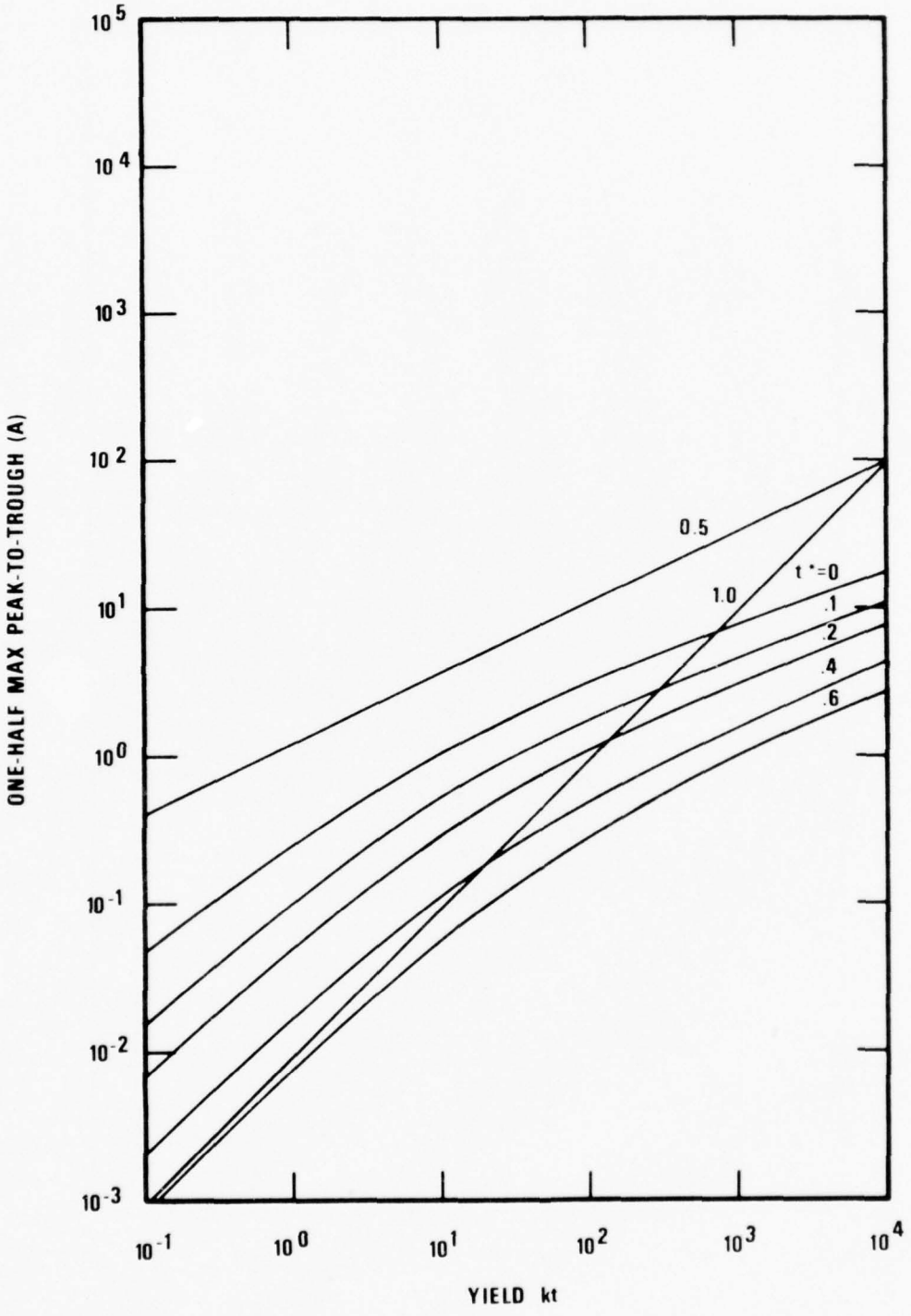

Figure 7c. Theoretical amplitude-yield curves for t*=0, 0.1, 0.2, 0.4, 0.6; tuff, one-half maximum peak-to-peak amplitude of signal, no surface reflection.

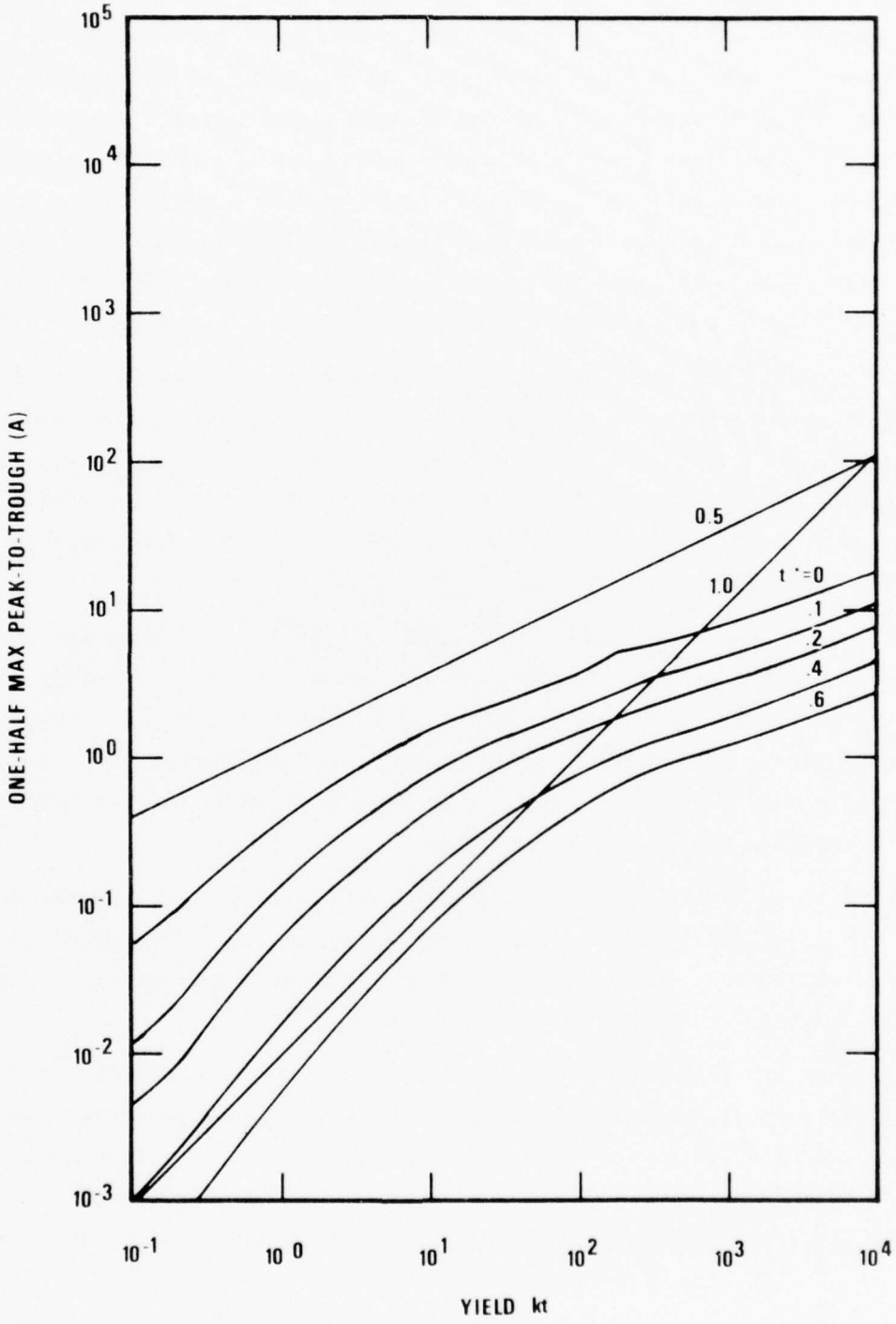

Figure 7d. Theoretical amplitude-yield curves for t*=0, 0.1, 0.2, 0.4, 0.6; tuff, one-half maximum peak-to-peak amplitude of signal, with surface reflection.

In Figures 7e and 7f we have computed amplitude as log(A/T) where A is the same as in Figures 7c,d except that it has been corrected for the system response at the period T. T is measured as the interval between the first zero crossings on either side of the maximum peak-to-trough amplitude. The curves in these figures are more irregular than in the preceeding ones because a large change in the period can occur with a small change in signal waveform, depending upon whether a "false cycle" crosses the zero line. This result would seem to indicate that for purposes of magnitude-yield estimation it would be best not to measure period or to correct A for it.

Measurement in the spectral domain at a selected frequency would result in the same amplitude-yield slope for any t*. (A white spectrum would result in a slope of 1.0 for any t*.) Care would have to be taken, however, to avoid the nulls, if any, created by pP interference. A possible solution here would be to compute the envelope of the spectrum. These are subjects for further research.

Figures 7g-l are similar to Figures 7a-f except that they are calculated with the granite reduced displacement potential. The low-frequency limit of this potential has been set equal to that of the tuff potential as a matter of convenience. The observed (granite/tuff) low-frequency ratio, Haskell (1967), is 0.49. From von Seggern and Blandford (1972) the parameters for 5 kt in granite are B = 2.04, k = 16.8.

By use of Figure 7m we may compare the granite and tuff curves and note that the granite curves maintain a slope close to 1.0 to higher yields than do the tuff curves, in accordance with a higher corner frequency for granite. Figure 7n gives curves for t*=0, 0.5, 1.0, 1.5, and 2.0.

Let us now compare some of these results with observation. In Figure 8 we see that for granite and with t* = 0.4 there is good agreement between theory and observation for the average teleseismic first motion ratios for LONGSHOT, MILROW, and CANNIKIN. The first motion data were reported by von Seggern and Blandford (1972). M_s ratios were also determined by von Seggern and Blandford, while the absolute level required for M_s estimation was determined by von Seggern and Lambert (1972). von Seggern and Blandford

---

von Seggern, D. H. and D. G. Lambert, 1972, Analysis of teleseismic data for the nuclear explosion MILROW, Seismic Data Laboratory Report 258, Teledyne Geotech, Alexandria, Virginia. AD 743 072.

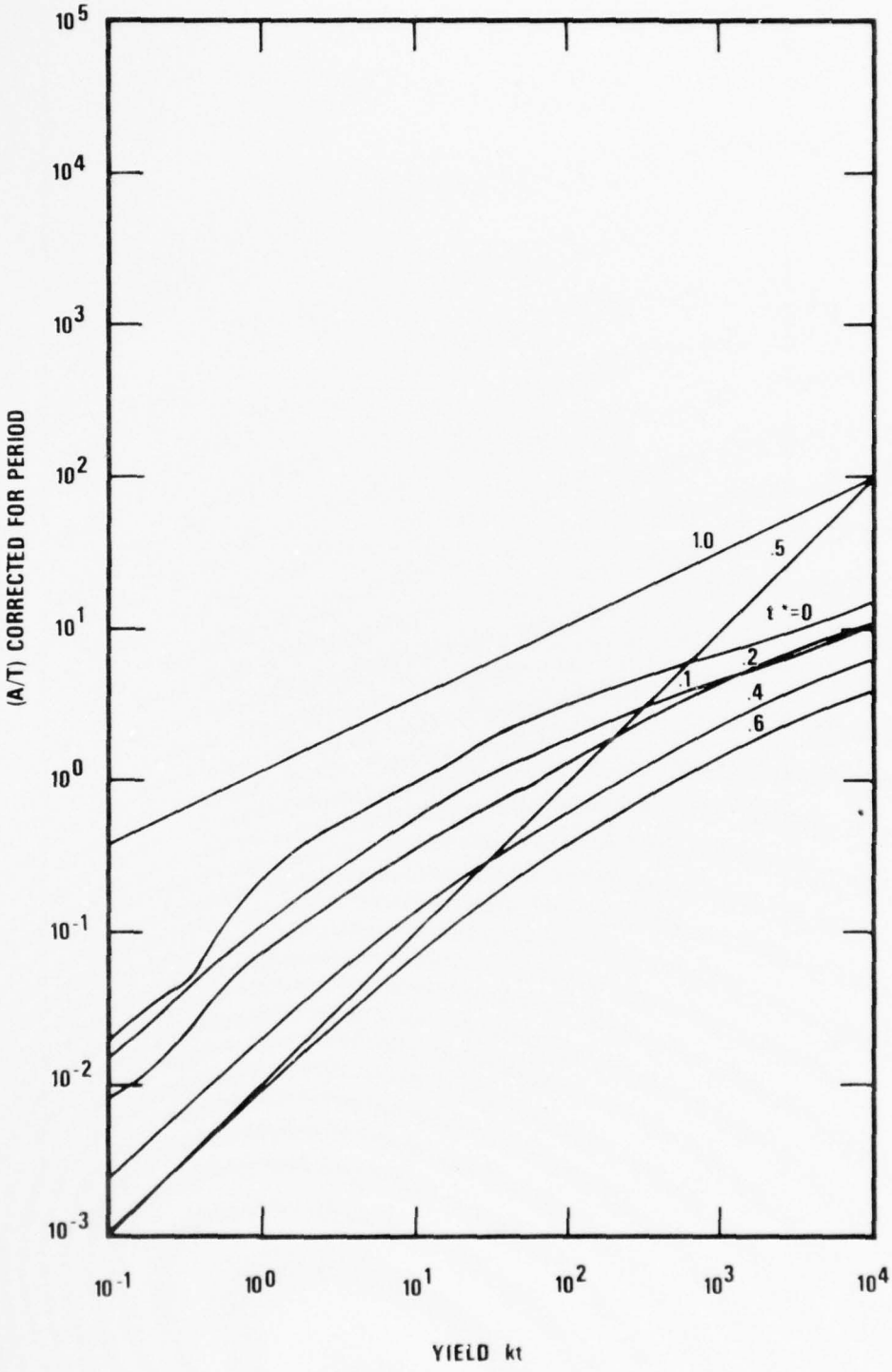

Figure 7e. Theoretical amplitude-yield curves for t*=0, 0.1, 0.2, 0.4, 0.6; tuff, (A/T) where A is one-half maximum peak-to-peak motion in the signal, corrected for system response at period T. T is measured as the time between zero-crossings on either side of the maximum peak-to-peak motion selected for measurement, no surface reflection.

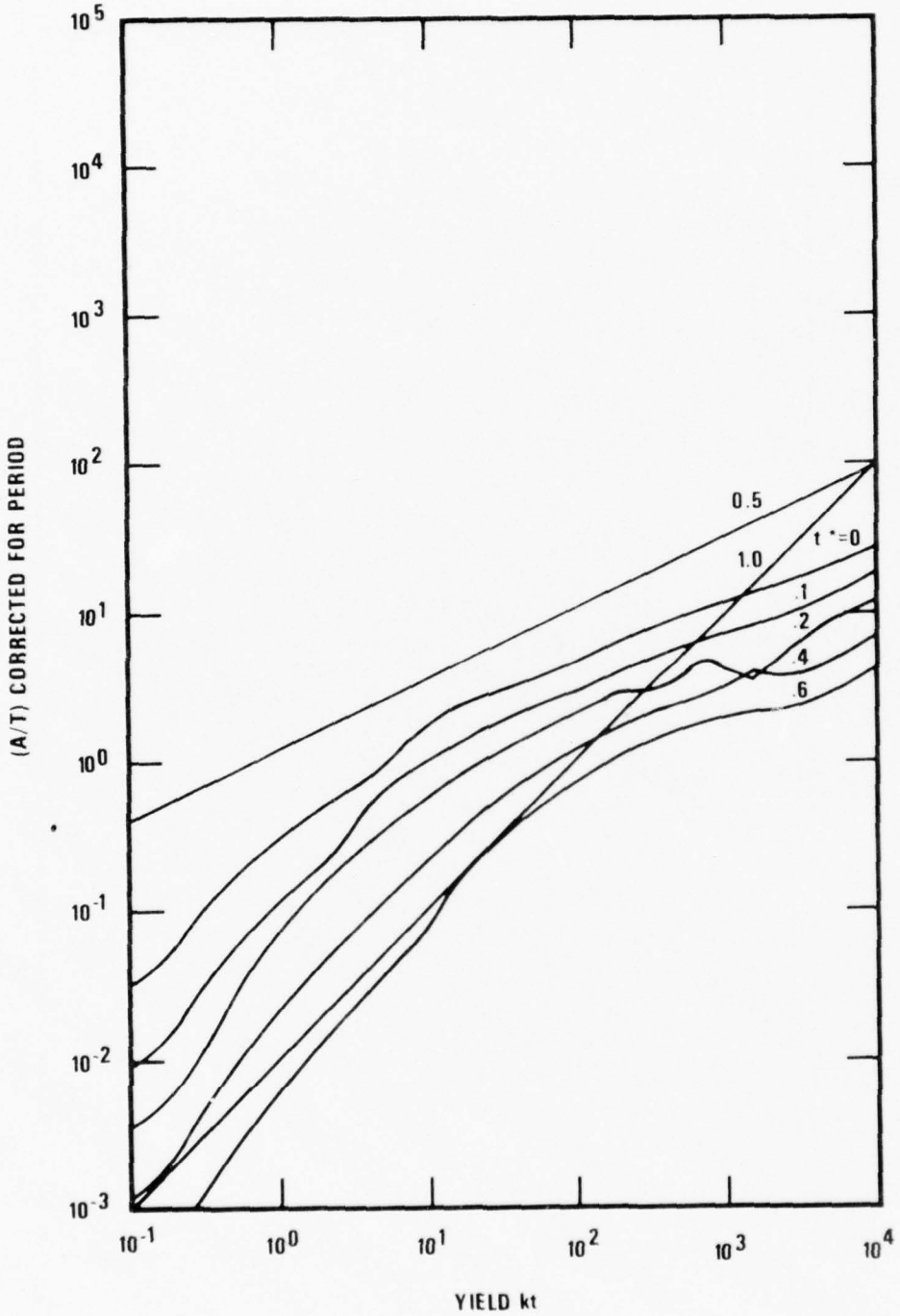

Figure 7f. Theoretical amplitude-yield curves for t*=0, 0.1, 0.2, 0.4, 0.6; tuff, (A/T) where A is one-half maximum peak-to-peak motion in the signal, corrected for system response at period T. T is measured as the time between zero-crossings on either side of the maximum peak-to-peak motion selected for measurement, no surface reflection.

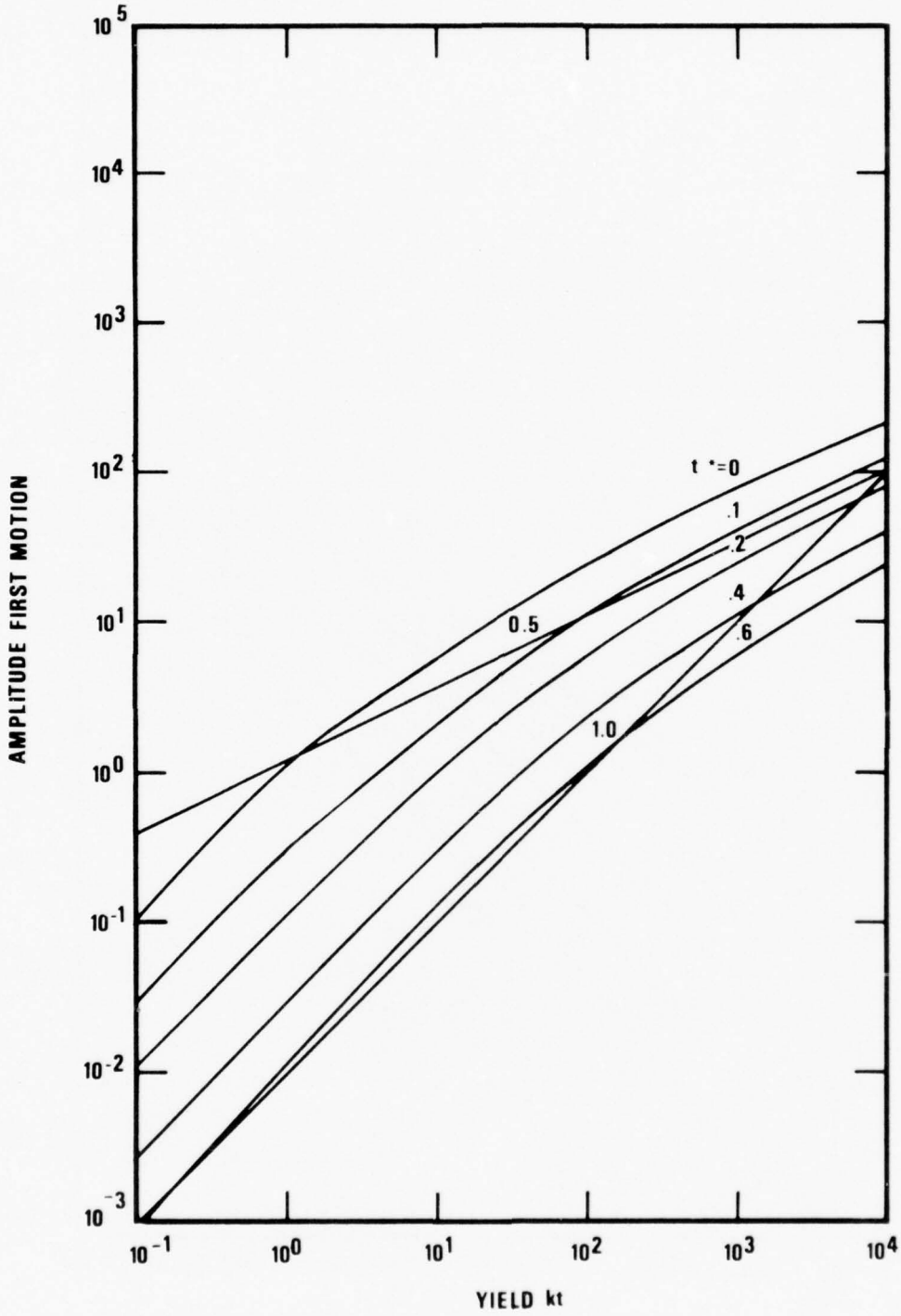

Figure 7g. Theoretical amplitude-yield curve for t*=0, 0.1, 0.2, 0.4, 0.6; granite, amplitude of first motion, no surface reflection.

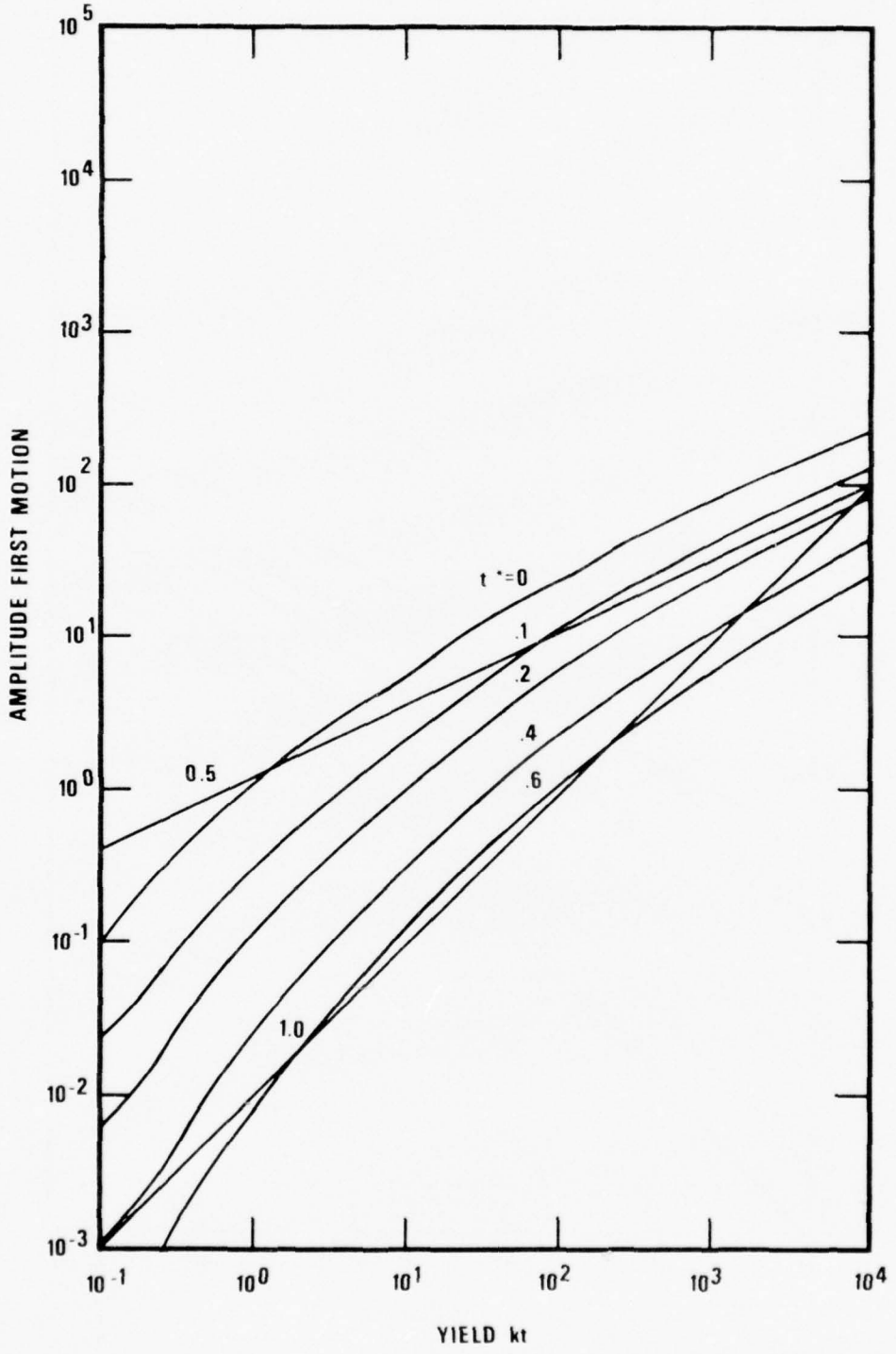

Figure 7h. Theoretical amplitude-yield curves for t*=0, 0.1, 0.2, 0.4, 0.6; granite, amplitude of first motion, with surface reflection.

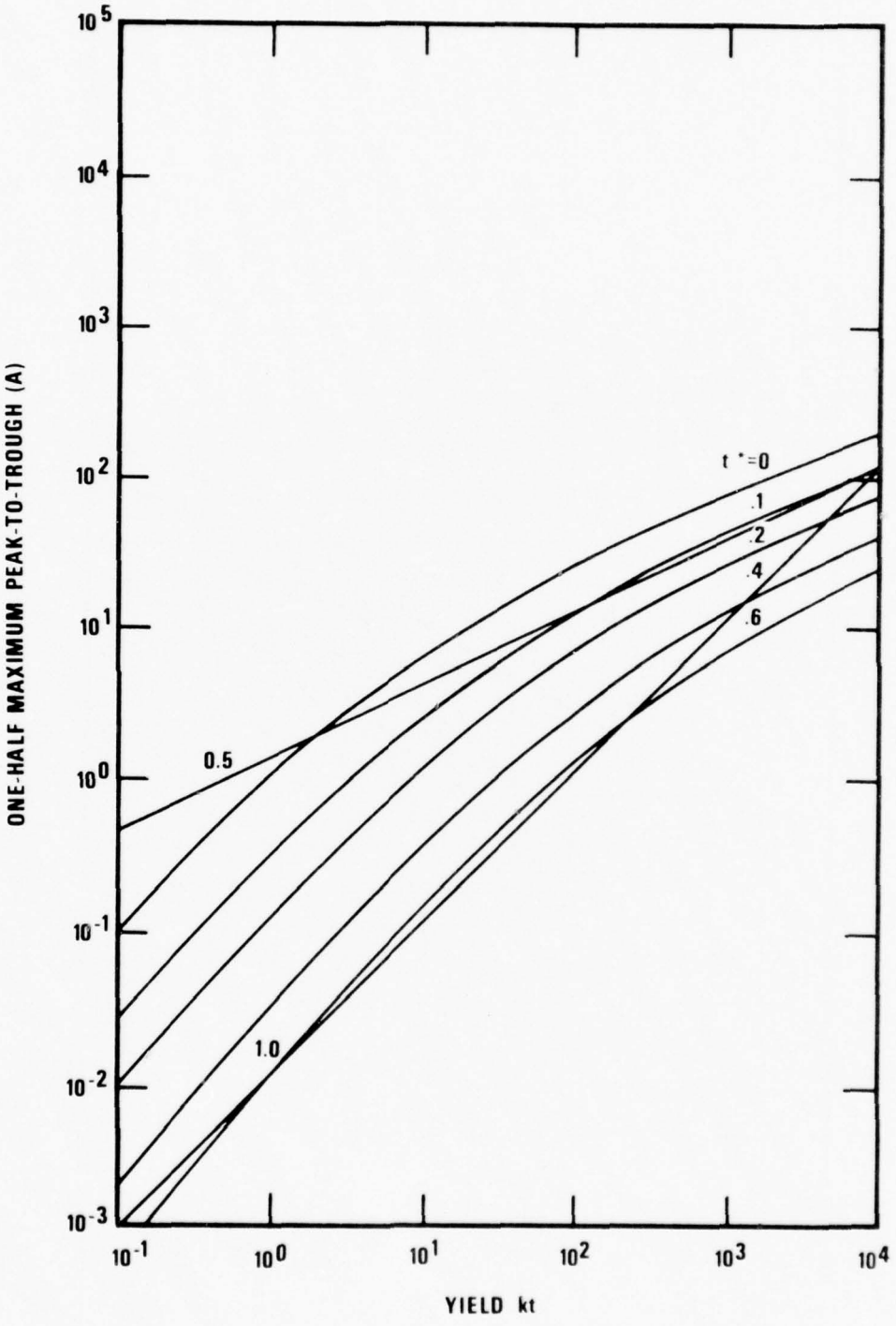

Figure 7i. Theoretical amplitude-yield curves for t*=0, 0.1, 0.2, 0.4, 0.6; granite, one-half maximum peak-to-peak amplitude of signal, no surface reflection.

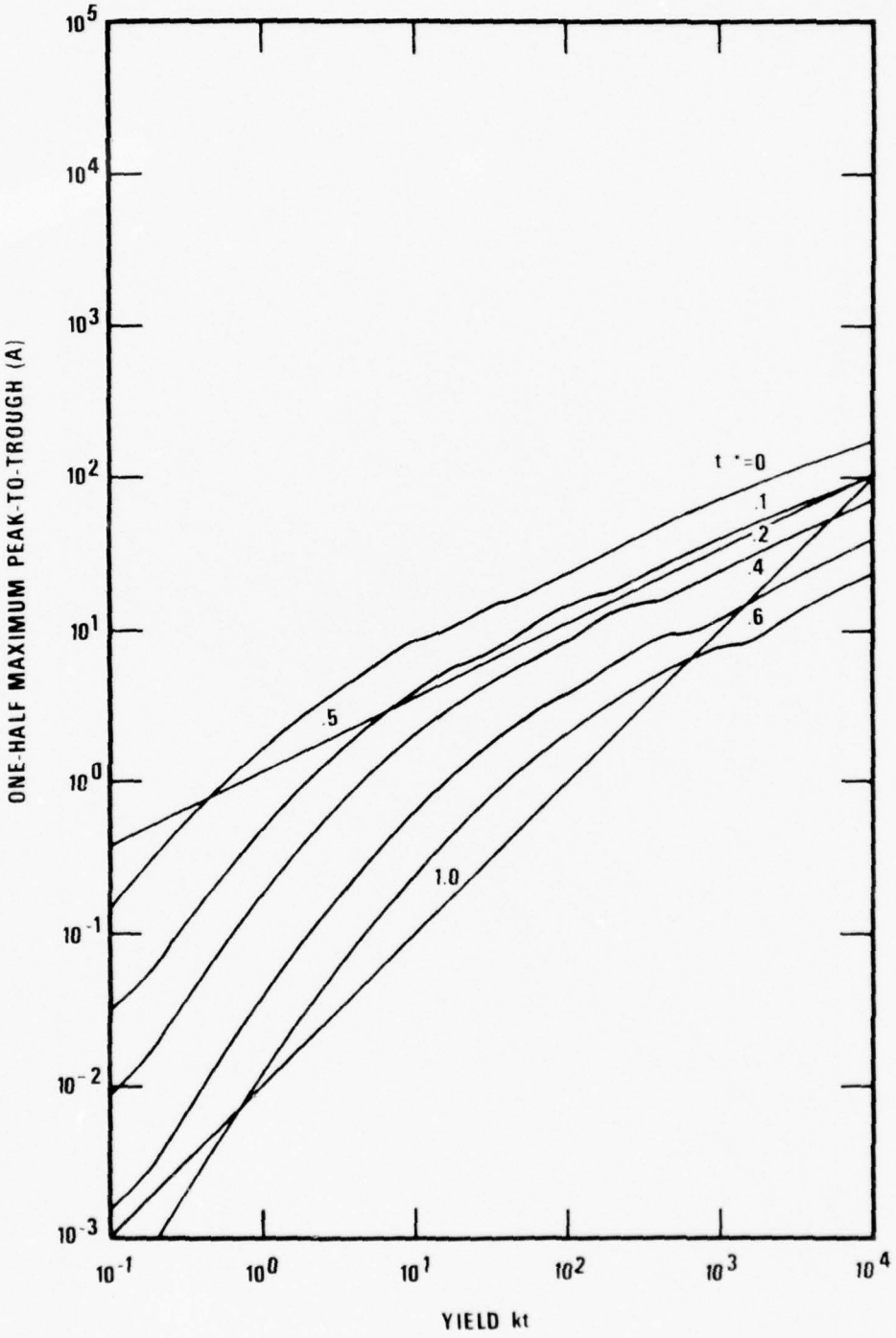

Figure 7j. Theoretical amplitude-yield curves for t*=0, 0.1, 0.2, 0.4, 0.6; granite, one-half maximum peak-to-peak amplitude signal, with surface reflection.

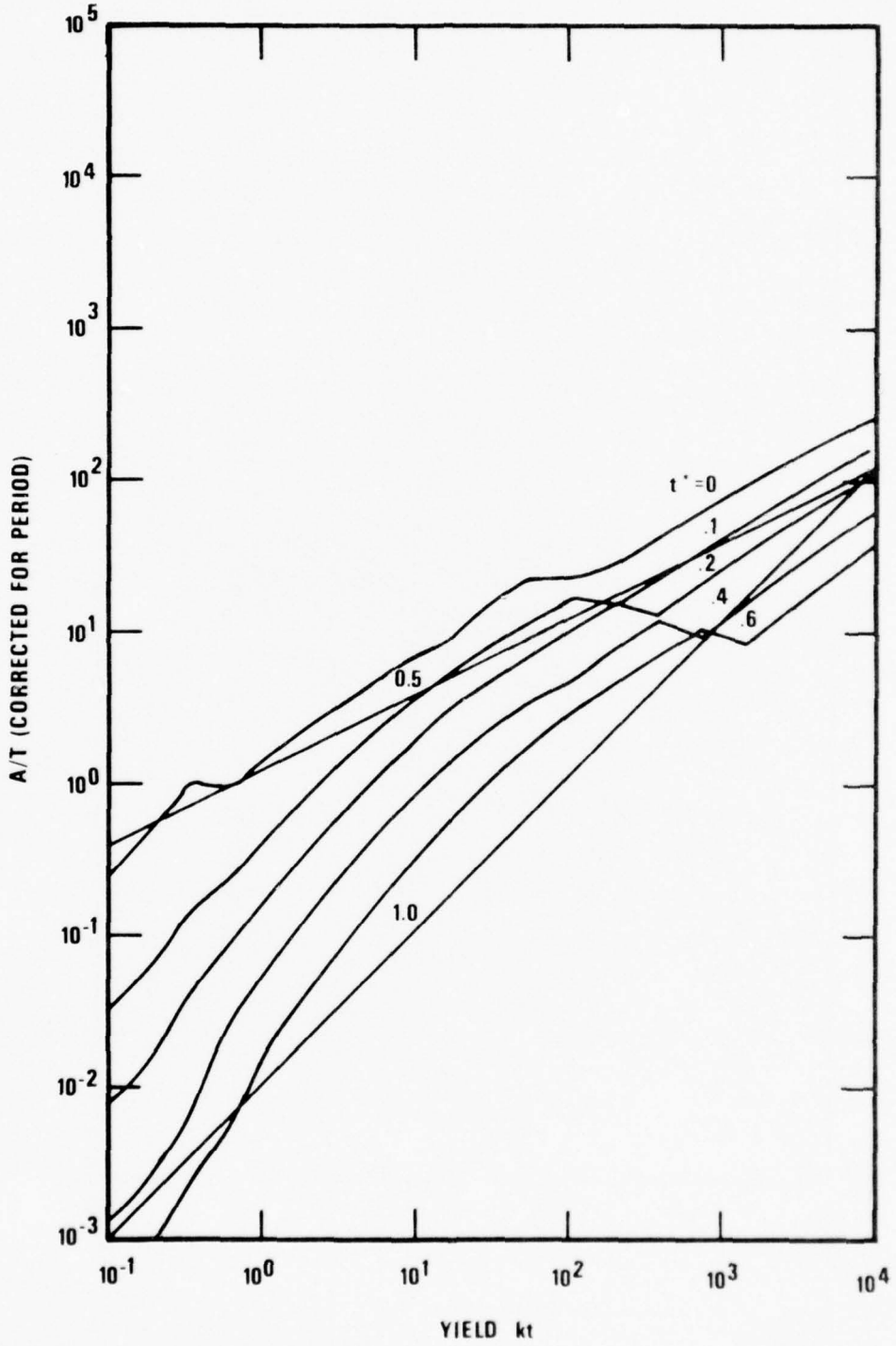

Figure 7k. Theoretical amplitude-yield curves for t*=0, 0.1, 0.2, 0.4, 0.6; granite (A/T) where A is one-half maximum peak-to-peak motion in the signal, corrected for system response at period T. T is measured as the time between zero-crossings on either side of the maximum peak-to-peak motion selected for measurement, no surface reflection.

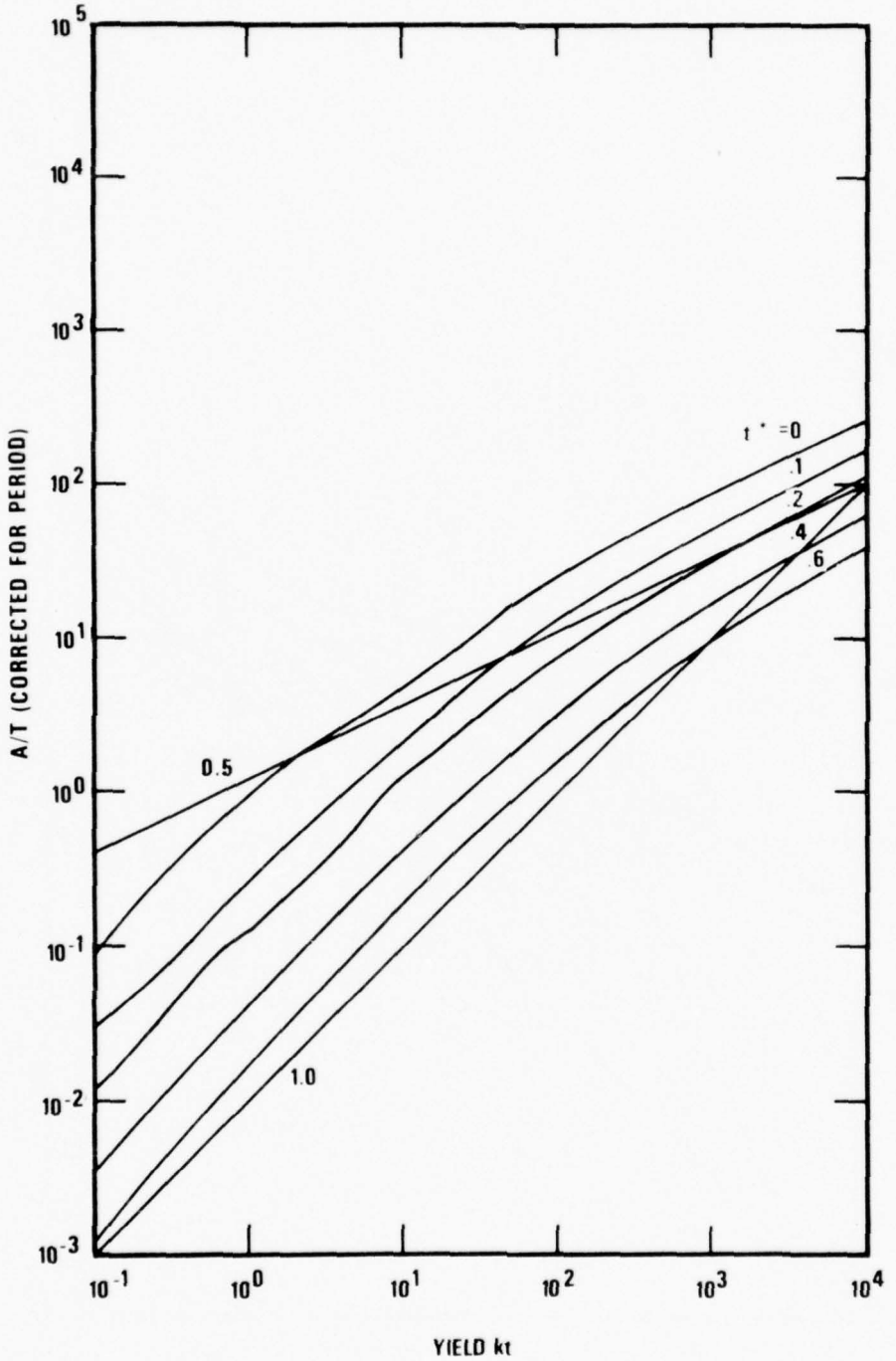

Figure 71. Theoretical magnitude-yield curves for t*=0, 0.1, 0.2, 0.4, 0.6; granite, (A/T) where A is one-half maximum peak-to-peak motion in the signal, corrected for system response at period T. T is measured as the time between zero-crossings on either side of the maximum peak-to-peak motion selected for measurement, with surface reflection.

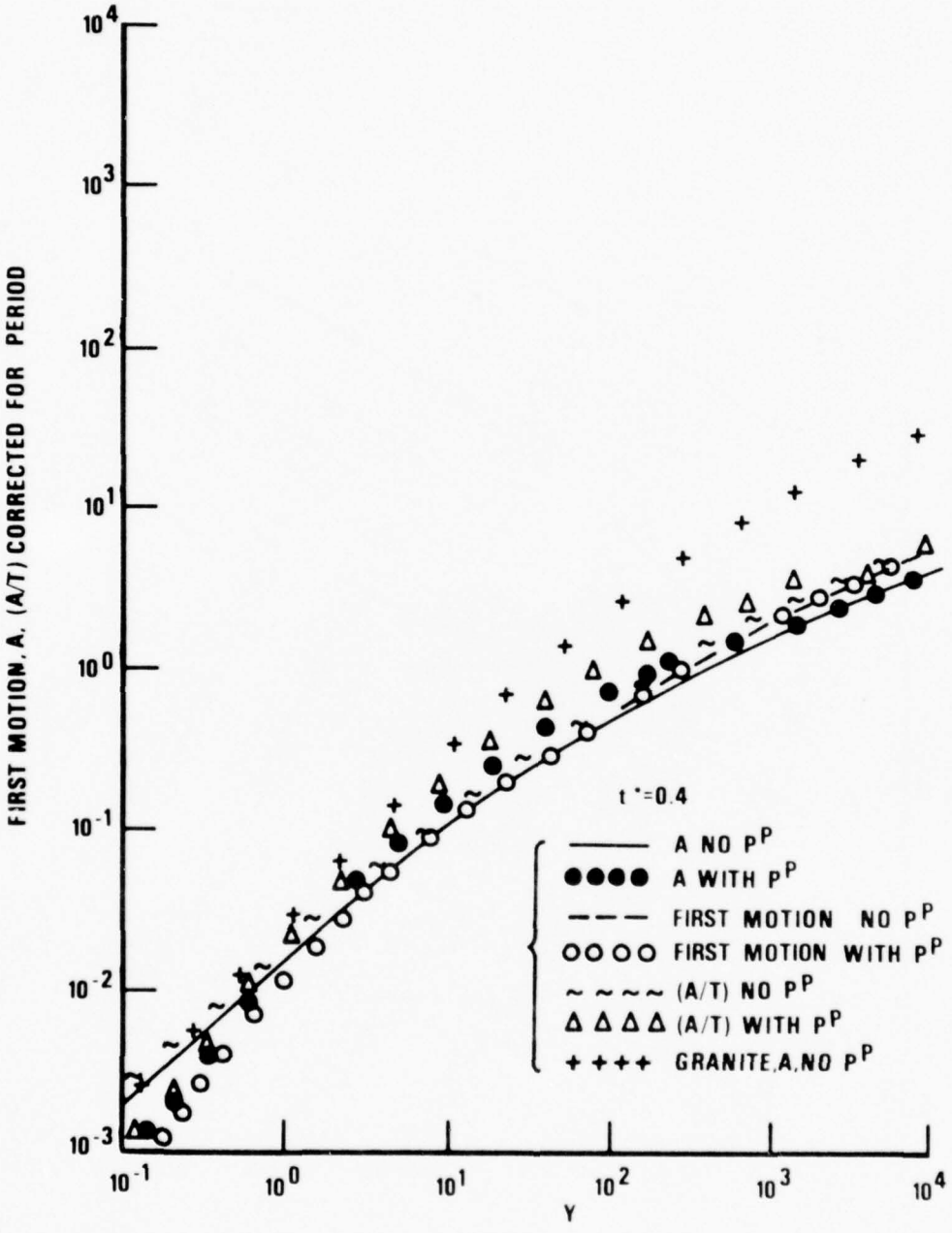

Figure 7m. Selected amplitude or magnitude-yield lines from Figures 7a-f, for tuff, plus one line for granite from Figure 7i.

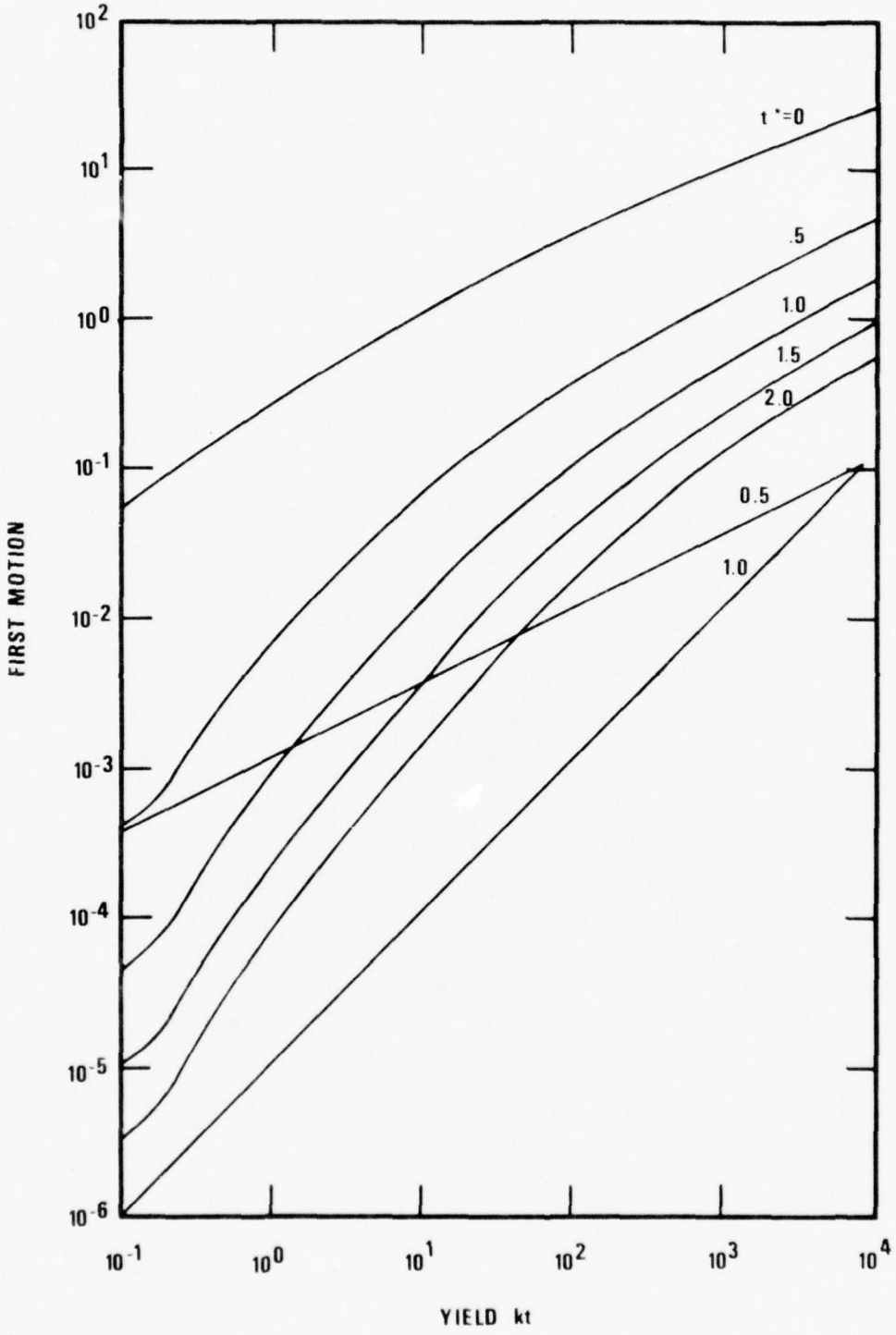

Figure 7n. Theoretical amplitude-yield curve for t*=0, 0.5, 1.0, 1.5, 2.0; tuff, amplitude of first motion, with surface reflection.

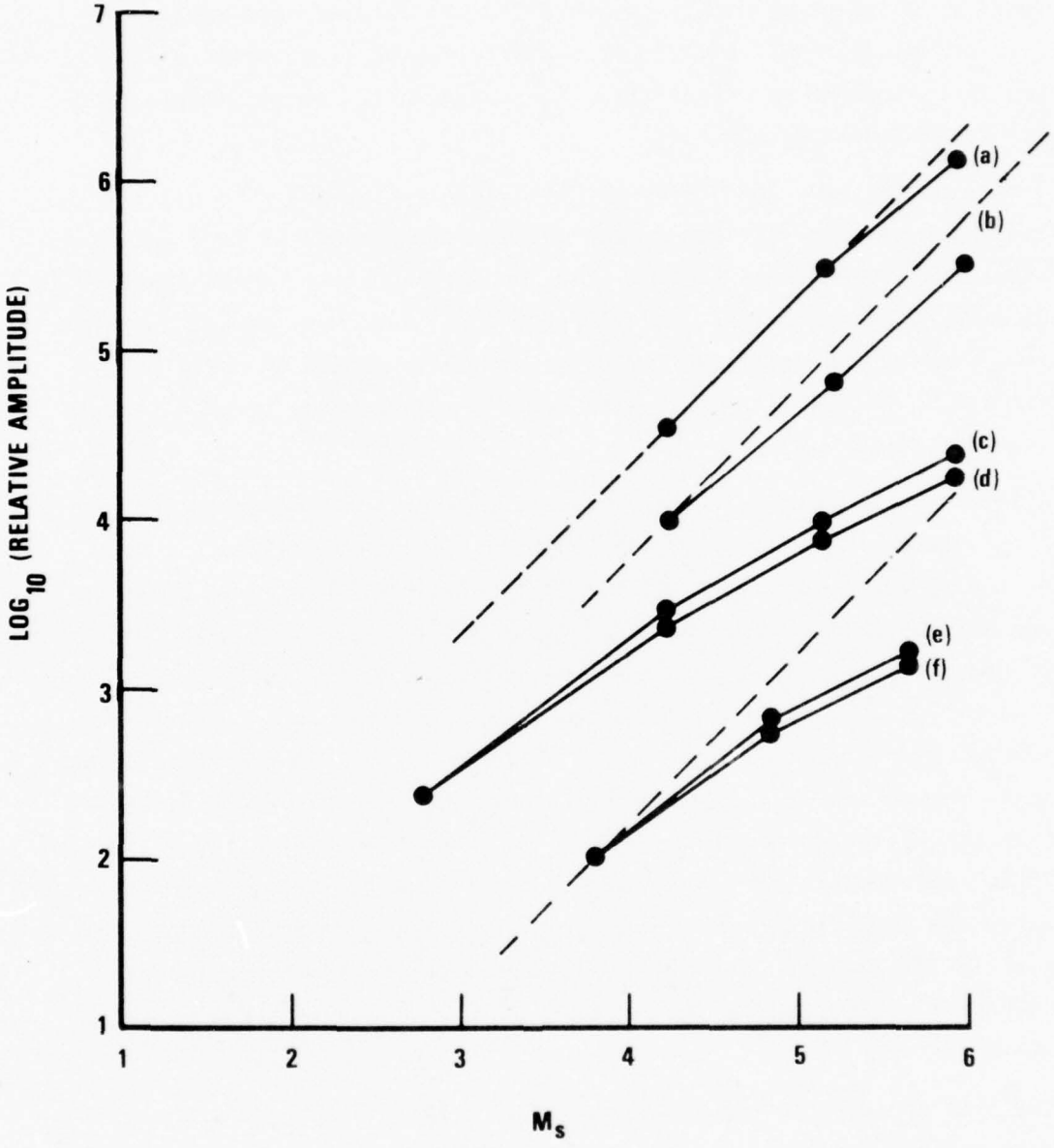

Figure 8. Four measures of short-period P-wave versus long-period LR radiation for the events BUTEO, REX, SCOTCH, and BENHAM. a) m_b (von Seggern, 1973); b) short-period NPNT first motion relative amplitude, log (REX amplitude) = 4; c) $\log_{10}$(a-b) mμ KNUT and MNNV; d) tuff theoretical relative first motion for 0.7, 19, 150, and 1100 kilotons, t*=0.1, fitted to first point of curve c; e) teleseismic first motion LONGSHOT, MILROW, CANNIKIN, von Seggern and Blandford (1972), M_S from von Seggern and Lambert (1972) and von Seggern and Blandford (1972); f) granite theoretical first motion ratio for 80, 1000, and 5000 kilotons; t*=0.4, fitted to first point of curve e.

also found good agreement simply by comparing the first-motion amplitude ratios to the predicted relative source amplitudes at 1 Hz. They also verified that the RKON spectral ratios for the Amchitka shots, corrected for pP, were in agreement with theory.

Similarly, we have good agreement with observation for t* = 0.1 for the relative first maximum to first-trough amplitudes measured at KNUT and MNNV for BUTEO, REX, SCOTCH, and BENHAM. The theoretical curve "d" in Figure 8 is for teleseismic first motion. Calculations for a head wave result in perfect agreement between the resulting new curve "d" and the data of curve "c". From earlier in this study we are also aware that agreement is excellent in the frequency domain.

A major contradiction arises, however, in attempts to compare theory with observations of teleseismic amplitude ratios. The m_b values for REX, SCOTCH, and BENHAM computed by von Seggern (1973) exhibit a slope close to 1.0, as do first motions measured especially for this study at NPNT. Apparently similar results are reported by Springer and Hannon (1973) in that they report slopes near 1.0 for teleseismic amplitude-yield observations of Pahute Mesa events below the water table. No value of t* in Figures 7a-f gives a curve which can be regarded as in agreement with a slope of 1.0. By reference to Figure 7n which gives first motions in tuff for t* values of 0, 0.5, 1.0, 1.5, and 2.0 we can see that a t* value of about 1.5 is needed to steepen and straighten the amplitude-yield curve between the teleseismically detectable limits of 10 and 1000 kt. Such a value is substantially greater than any ever suggested before, and is much greater than ever deduced from spectral analysis of data.

The only apparent escape from this paradox is to assume that the effective reduced displacement potential is different for waves departing nearly vertically downward than for those departing upward or sideways. The rays measured for reduced displacement potentials and regional observations emerge in these latter directions. A substantially higher value of k, say k=30 instead of k=12, would straighten out the curve for values of t* = 0.5. Aside from measurements taken simultaneously just outside the elastic zone below and to the side of an explosion, the only direct way of approaching this problem would seem to be hydrodynamical numerical calculations to verify the differences as a function to takeoff angle. The differences presumably

would result from the varying effects of gravity at varying emergence angles, and thereby from the resistance of the mass of the earth at low emergence angles as compared to hydrostatic pressure at high emergence angles. The good agreement found above between the Amchitka teleseismic measurements and results predicted from a reduced displacement potential for granite may simply reflect the greater strength of Amchitka basalt as compared to NTS tuff. This greater strength would seem, intuitively, to reduce asymmetry due to hydrostatic pressure gradient.

We should keep in mind that the explosions considered in Figure 6 were all below the water table, whereas examination of typical water table levels for shots at Rainier Mesa (Springer and Kinnaman, 1971) indicates that RAINIER, from which the tuff potential was derived, was above the water table. This would suggest that the water mass fraction f_w, and the initial air-filled volume fraction ϕ_o would be different between RAINIER and the events in this report to which RAINIER's measured reduced displacement potential was applied. Furthermore the calculations of Cherry et al. (1975a,b) suggest substantial changes in the reduced displacement potential for plausible changes in ϕ_o and f_w. Thus it would seem to be coincidence that the RAINIER reduced displacement potential satisfactorily accounts for the rays departing BUTEO, REX, SCOTCH, and BENHAM to local distances.

Springer, D. L. and R. L. Kinnaman, 1971, Seismic source summary for U.S. underground nuclear explosions, 1961-1970, v. 61, p. 1073-1098.

DURYEA, AN EVENT AT THE WATER TABLE

In Figure 9 we see the spectral ratio DURYEA/BUTEO. There are a number of interesting features in this figure which can be explained by reference to the fact that DURYEA was set off just above the water table, so that the upgoing wave which was converted into pP and LR was probably less effectively coupled than the downgoing direct P. It is noteworthy that use of k_o=10, α=0.2 for DURYEA gives a better fit than the standard k_o=12, α=0.5. The difference, though small, can be detected with some confidence. This implies less high frequency energy and a small pP and would seem to be consistent with the idea that the shallow tuff layers are more porous than the deeper ones. Frasier (1972) also concluded that pP phases from NTS explosions were of lower amplitude and frequency than P.

Note also in Figure 9 that the LR ratio, obtained using the DURYEA M_s from von Seggern (1973), is substantially less than the yield ratio; and is lower (0.5 magnitude units) by about the degree of the estimated ratio (0.7/0.2) of pP amplitudes. Thus one might expect that NTS explosions tested right at the water table might be easier to discriminate than shallower or deeper ones. On the other hand, the influence of a weak pP on m_b must also be considered, since we have seen that for intermediate yield events a strong pP can enhance m_b by 0.2 magnitude units.

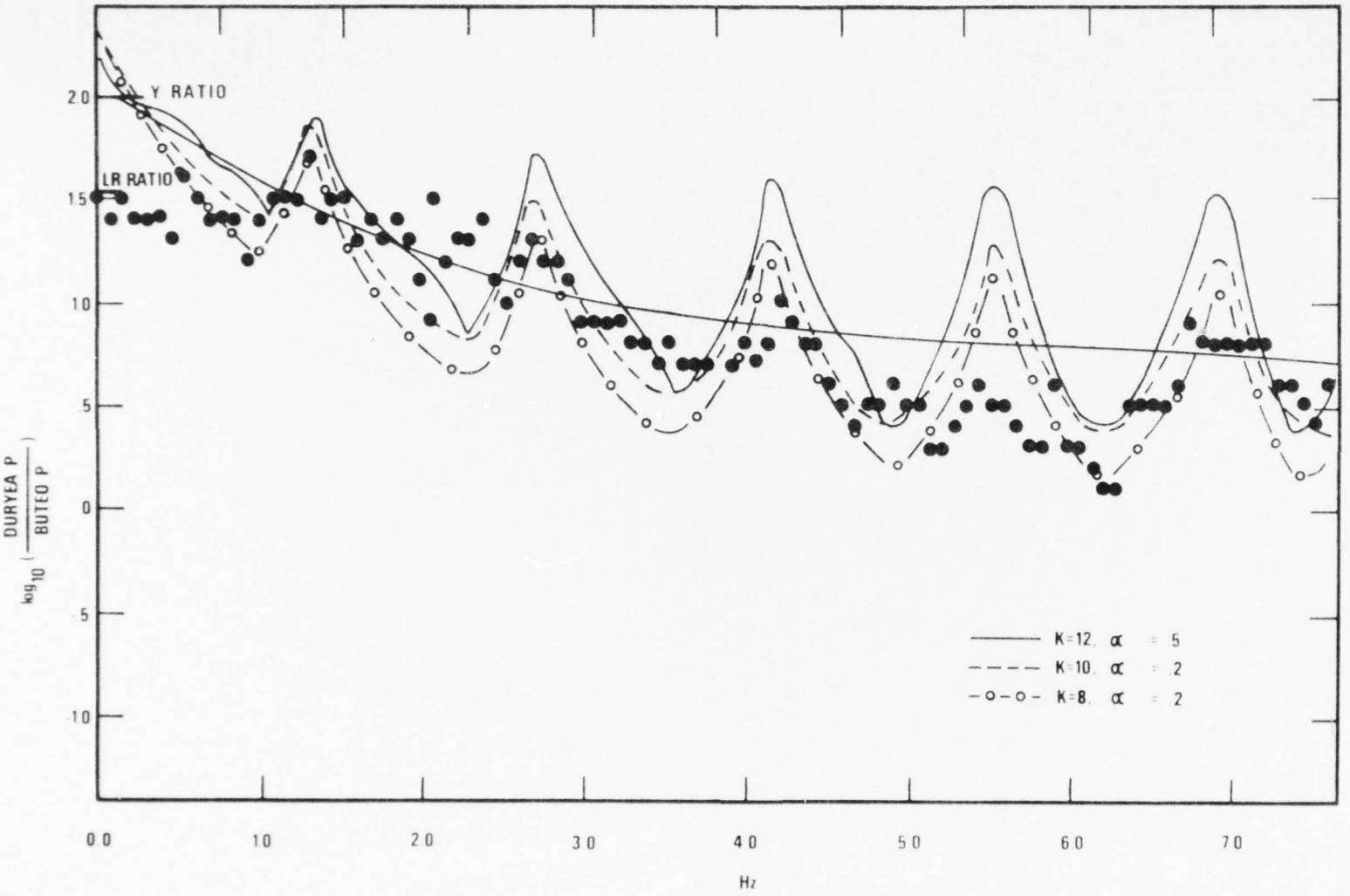

Figure 9. Spectral ratio DURYEA/BUTEO.

CRATERING EXPLOSIONS

Figure 10 shows the KNUT SPZ traces for the cratering explosions considered in this report, together with the trace for PAR, a contained explosion in alluvium which we shall compare with the cratering explosion SEDAN, exploded nearby and in similar material. We notice immediately as can be verified by inspection of the spectra in Figure 11 that the contained event, PAR, is apparently of lower frequency than the cratering event, SEDAN, which is also of greater yield. This seems contrary to intuitive expectations. We shall see below that this actually reflects the absence in SEDAN of intermediate frequencies.

In the cratering series PALANQUIN, CABRIOLET, SCHOONER (all events near to one-another), SCHOONER has the highest yield and the lowest frequency, which is in general agreement with intuitive expectations.

In Figure 12 we see the LR data for these events as recorded at MNNV. Non-linear behavior is apparent for the recording of the SCHOONER event, as we saw also for the REX event. Relative measurements were also made on LR at KNUT for these events, and for none of them was there any indication of non-linearity. Taking care to measure only common, undistorted phases the following LR $\log_{10}$ amplitude ratios to BUTEO were determined: CABRIOLET, -0.37; PALANQUIN, -0.24; SCHOONER, 1.15. The value for SEDAN/PAR was determined to be 1.08. These values are entered at zero frequency on the spectral ratio plots which follow.

Figure 13a gives the spectral ratio of SEDAN/PAR, a cratering shot as compared to a contained shot, both in dry alluvium. We note that the high-frequency, and possibly the low-frequency, P-wave amplitude ratio is approximately equal to the yield ratio. Between 1.0 and 3.0 Hz, however, SEDAN has considerably less energy than would be expected from the yield ratio. The LR ratio is substantially greater than the yield ratio. This null in the intermediate frequencies for SEDAN (or maximum in intermediate frequencies for PAR) accounts for the apparently lower frequency content for PAR in the time domain. From these results one might hazard as generalities that the high-frequency radiation for all types of shots in alluvium will be in proportion to yield, while the LR will be substantially greater for the cratering shots.

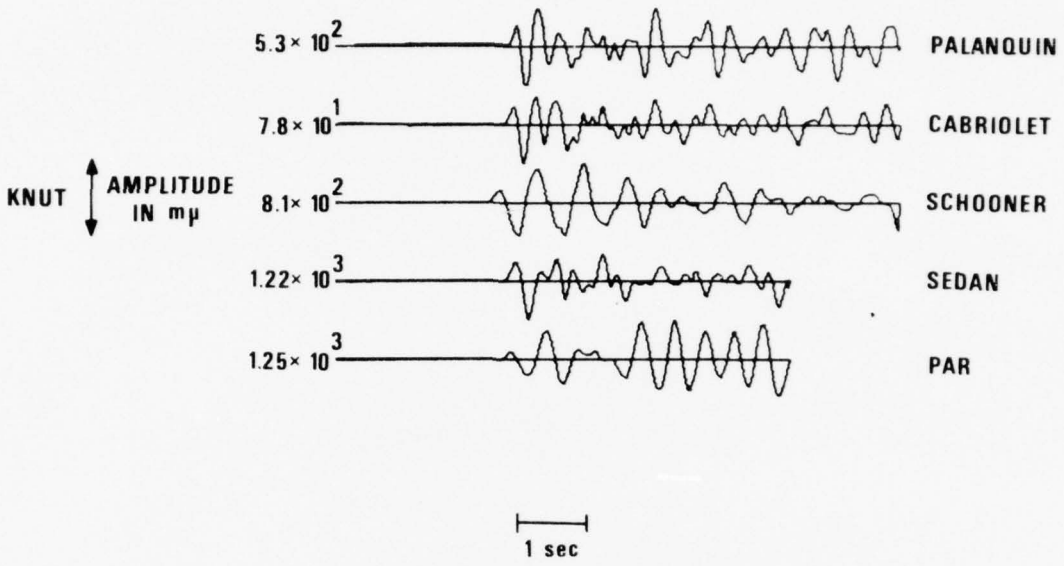

Figure 10. First few seconds of SPZ data as recorded at KNUT for events PALANQUIN, CABRIOLET, SCHOONER, SEDAN, and PAR. All except PAR were cratering events.

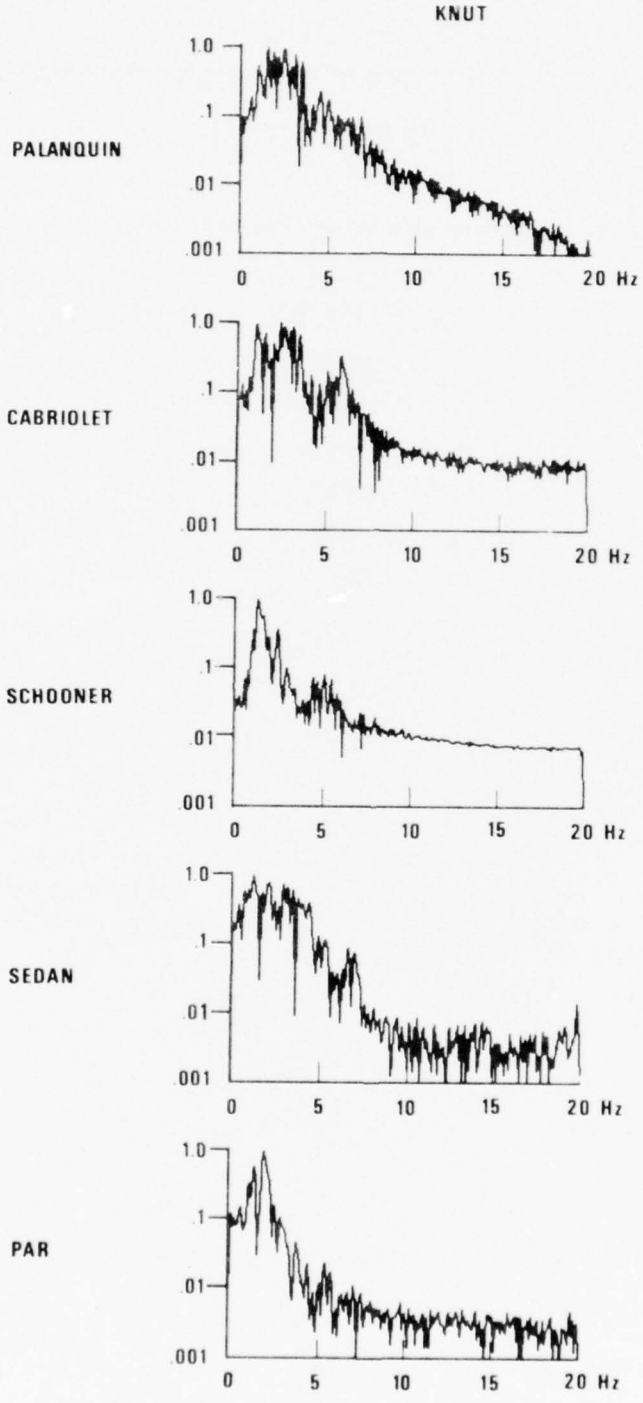

Figure 11. Log-amplitude spectra of KNUT data plotted in Figure 10.

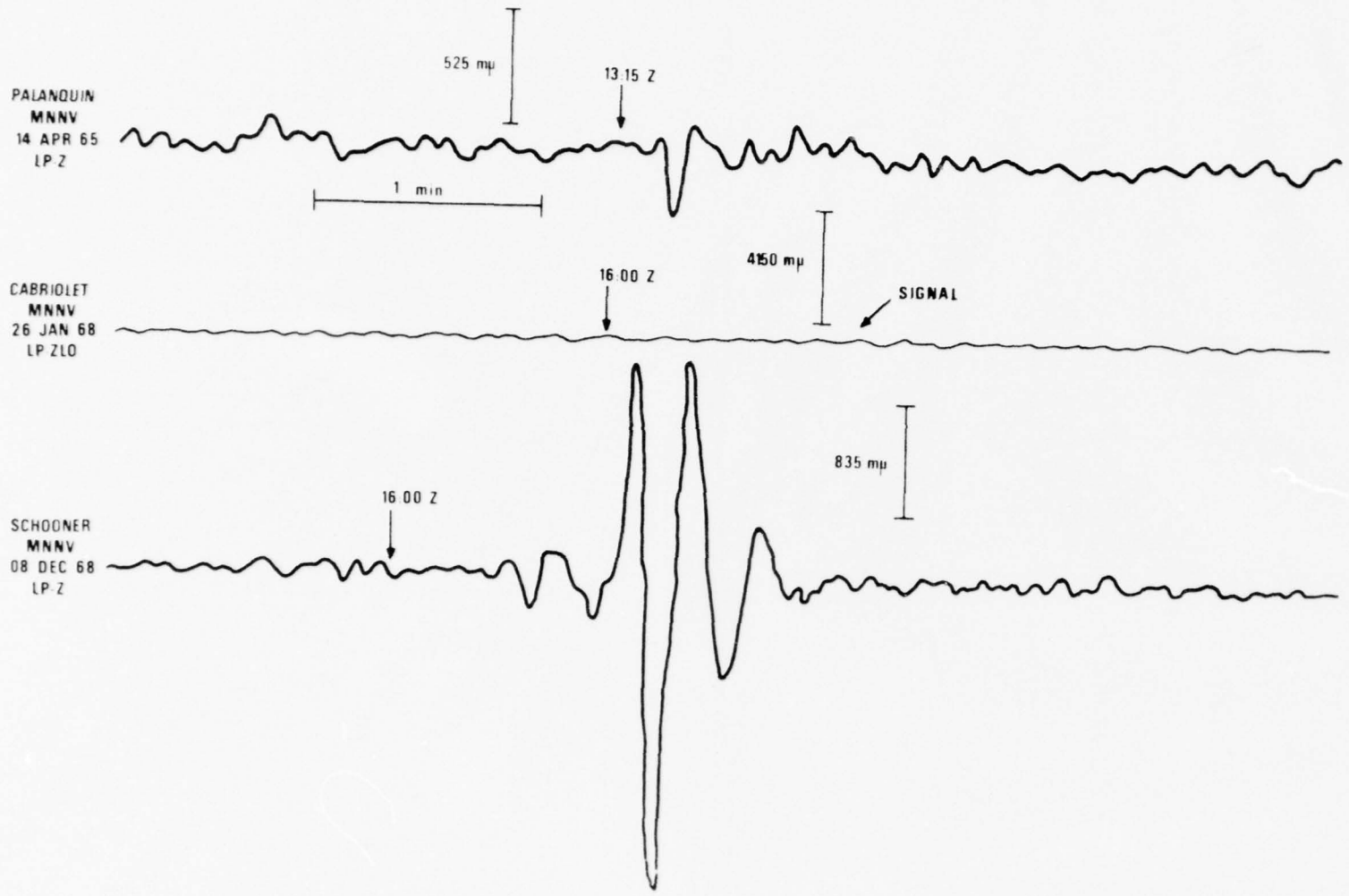

Figure 12. Long-period waveforms at MNNV for the events in Figure 10.

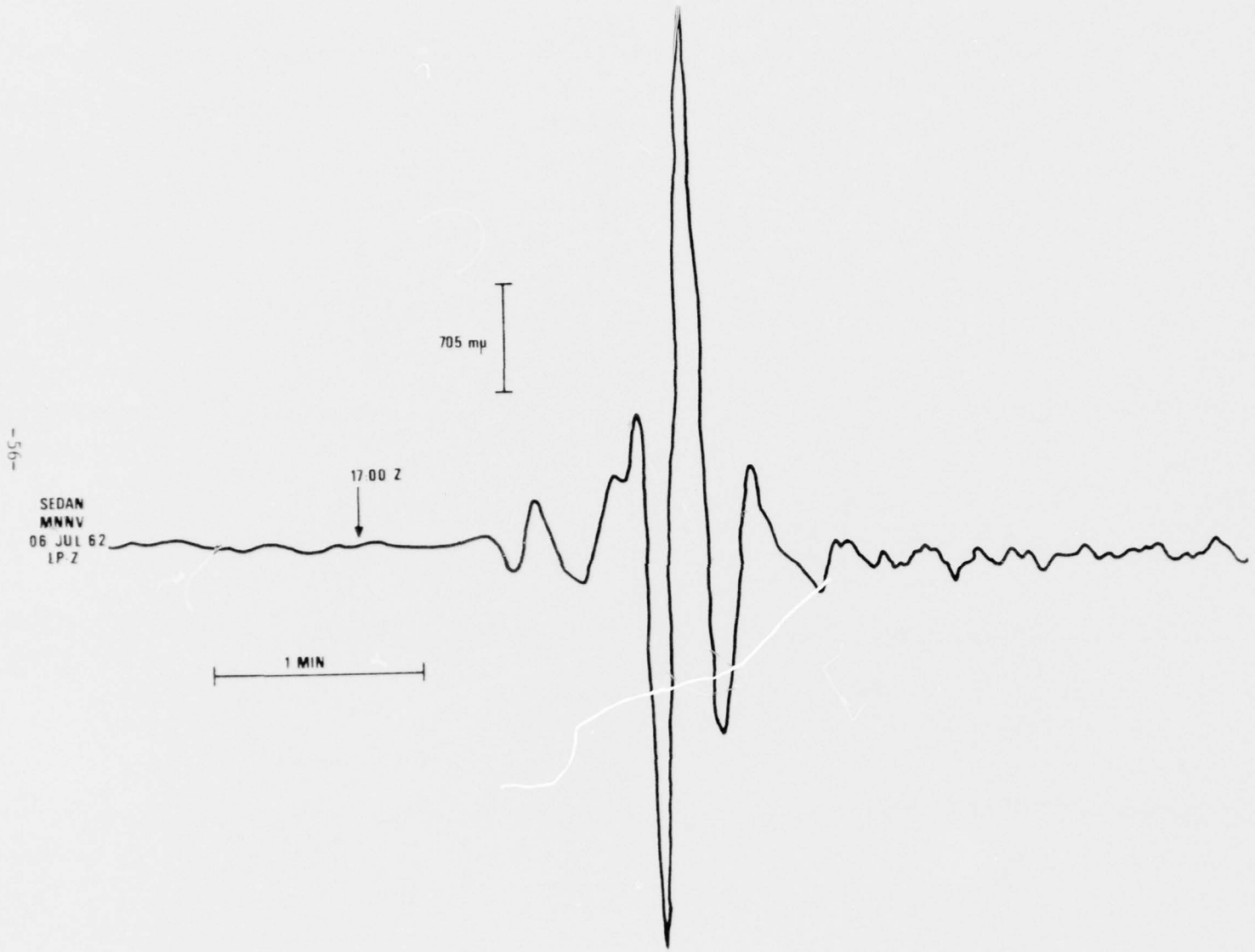

Figure 12 (Cont.). Long-period waveforms at MNNV for the events in Figure 10.

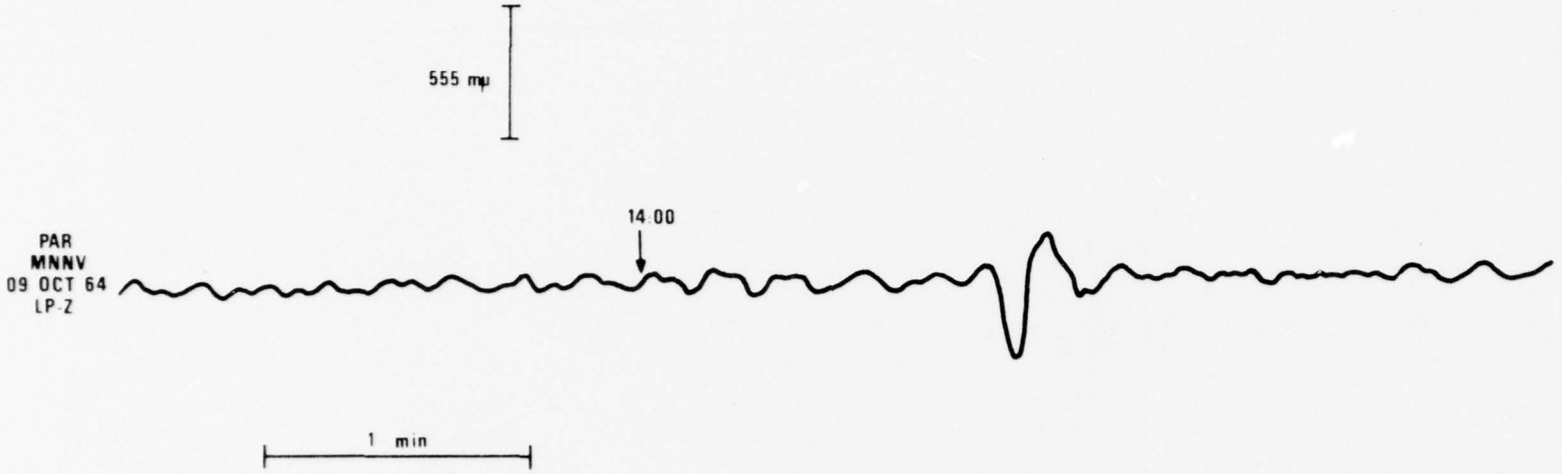

Figure 12 (Cont.). Long-period waveforms at MNNV for the events in Figure 10.

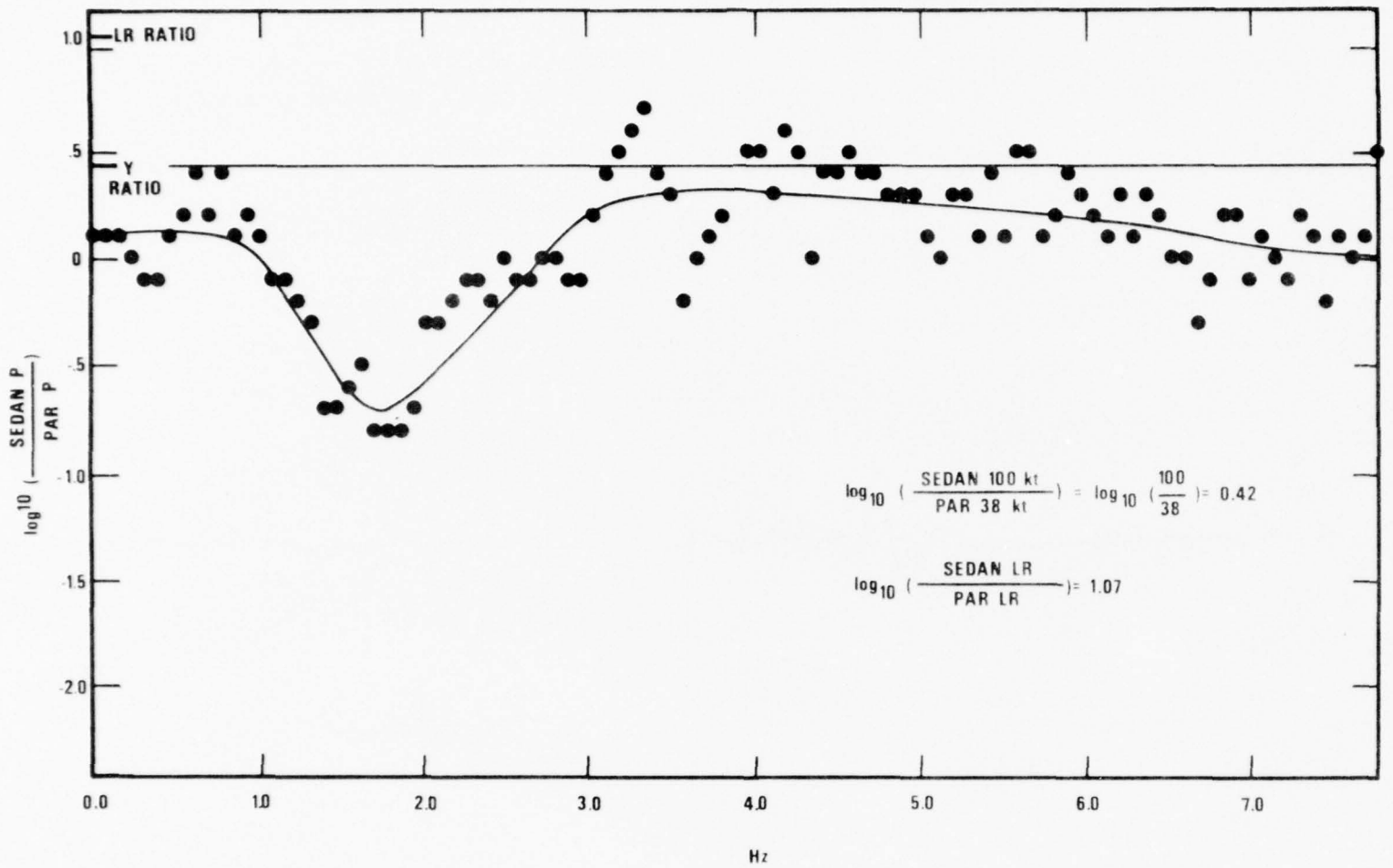

Figure 13a. Spectral ratios for cratering explosion: SEDAN/PAR.

In Figure 13b, SCHOONER/REX, we compare the spectrum of a buried shot in saturated tuff to a cratering shot in unsaturated tuff with both shots being of approximately equal yield. As would be expected, the amplitude ratio is less than the yield ratio at every frequency. In this case the LR ratio is less than the yield ratio. Apparently better coupling for the buried event in a more competent medium has overcome the tendency for the cratering explosion to more efficiently generate surface waves. A number of ratios of this type were presented by Mueller and Murphy (1971).

In Figure 13c, SCHOONER/DURYEA, we compare a cratering explosion to a buried explosion just at the water table. Here we find almost all frequencies equally well excited and in proportion to the yield, although, as with the previous two slides there is a frequency band, in this case from 1.5 to 4.5 Hz, where the cratering explosion seems to generate less efficiently.

Figures 13d, e, f compare the cratering explosions SCHOONER, PALANQUIN, and CABRIOLET to the overburied shot BUTEO. In each case at high frequencies, the cratering explosion has substantially less high frequency energy than does the buried explosion; and at all frequencies substantially less energy than indicated by the yield ratios. We must remember, however, that the explosions in these ratios are <u>not</u> in identical media; and this fact alone may account for most of the difference.

These last three figures have been computed to see if our knowledge of the BUTEO source function could be exploited to determine an equivalent reduced displacement potential for cratering explosions. Matching the theoretical and observed ratios was very difficult, since the low frequency asymptotes could not be predicted theoretically nor observed experimentally due to low S/N. Attempted matchings of the three observed and computed average spectral ratios implied that $1.0 \leq k_o \leq 4.0$ and $B < 8.0$. Thus, as might be expected, we find that the time constant for cratering explosions in dry tuff is larger than for a contained explosion in saturated tuff.

Mueller, R. A. and J. R. Murphy, 1971, Seismic characteristics of underground nuclear detonations: Part I, Seismic scaling law of underground detonations, Bull. Seism. Soc. Am., v. 61, p. 1675-1692.

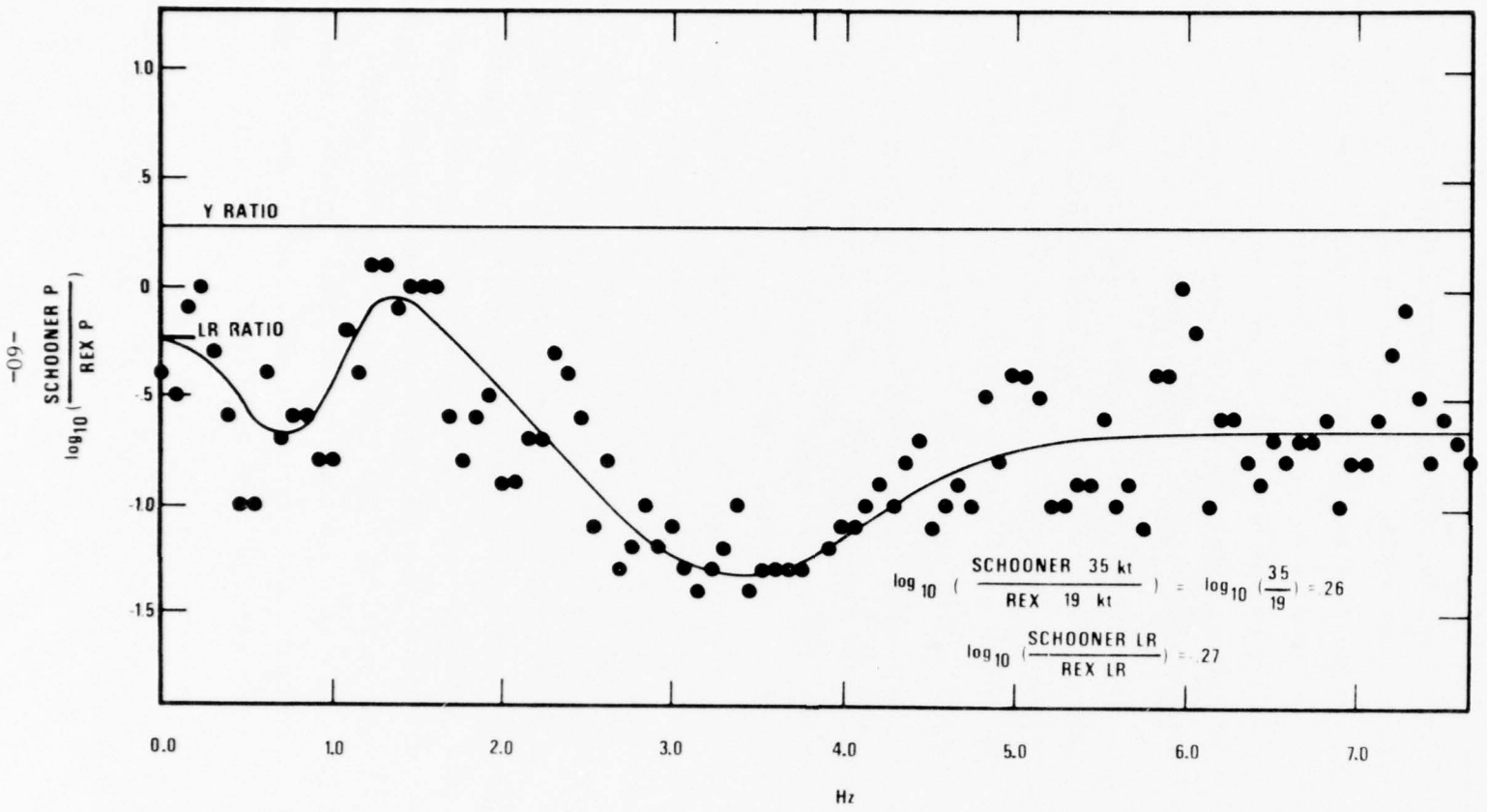

Figure 13b. Spectral ratios for cratering explosion: SCHOONER/REX.

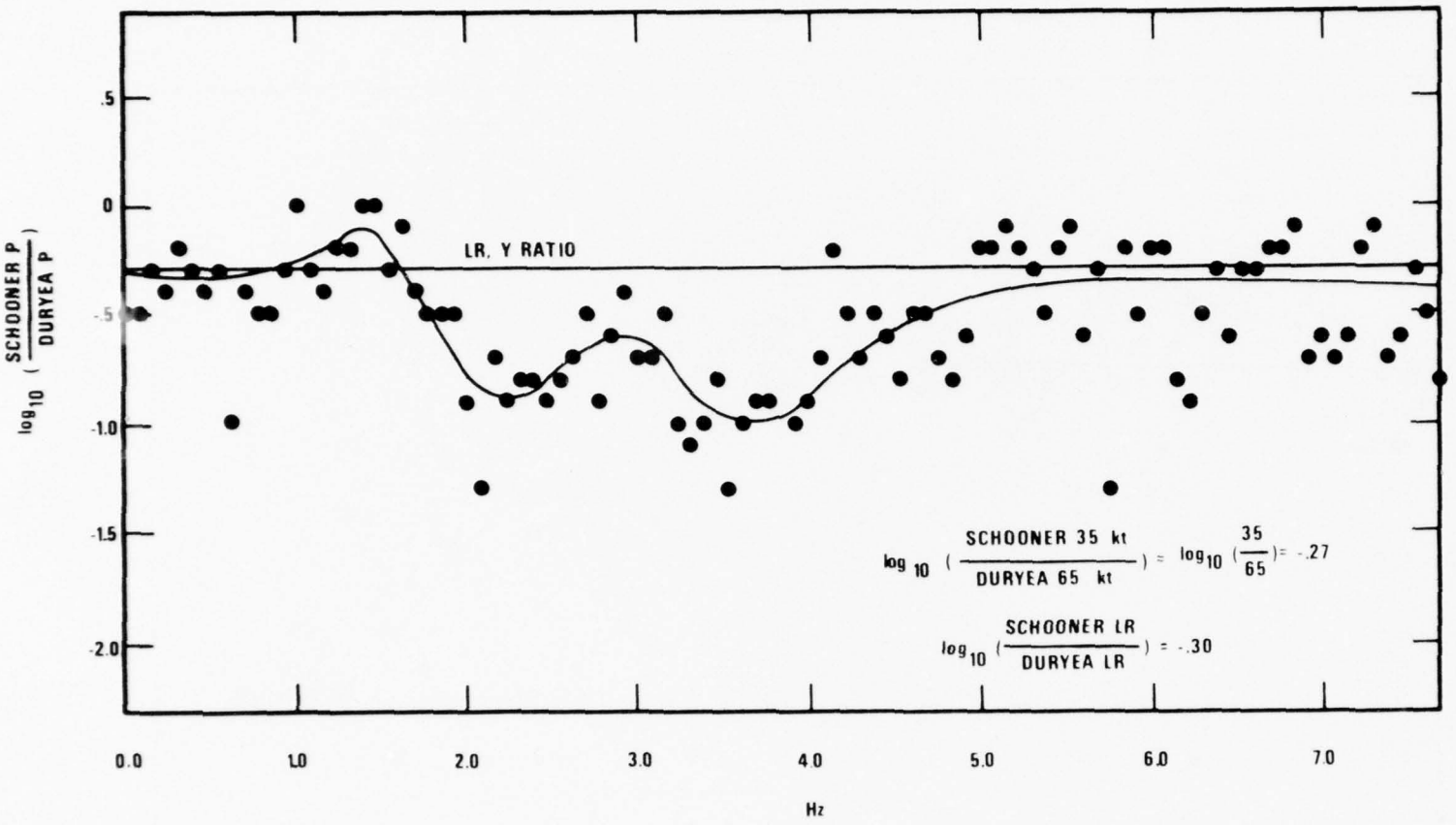

Figure 13c. Spectral ratios for cratering explosion: SCHOONER/DURYEA.

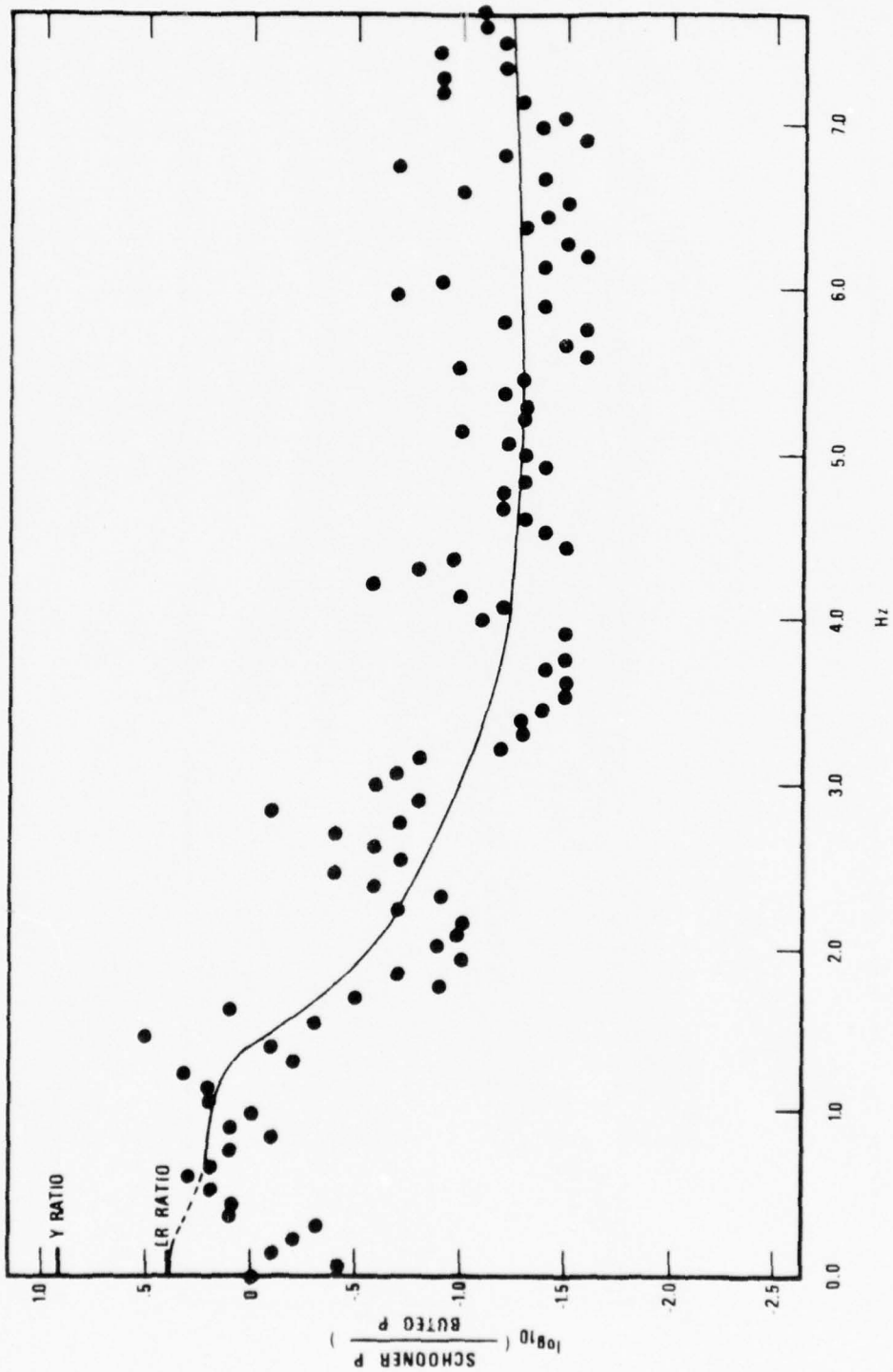

Figure 13d. Spectral ratios for cratering explosion: SCHOONER/BUTEO.

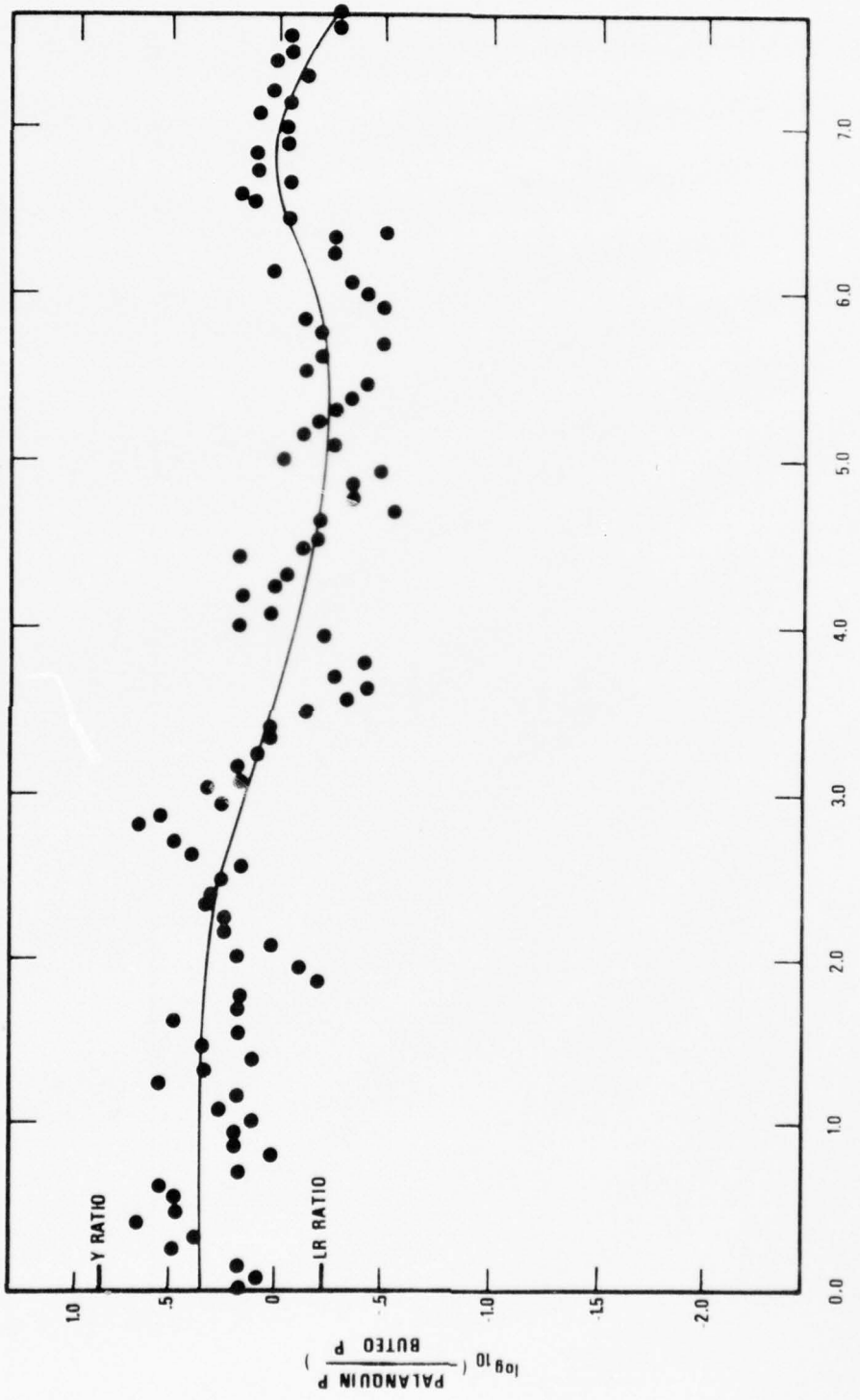

Figure 13e. Spectral ratios for cratering explosions: PALANQUIN/BUTEO.

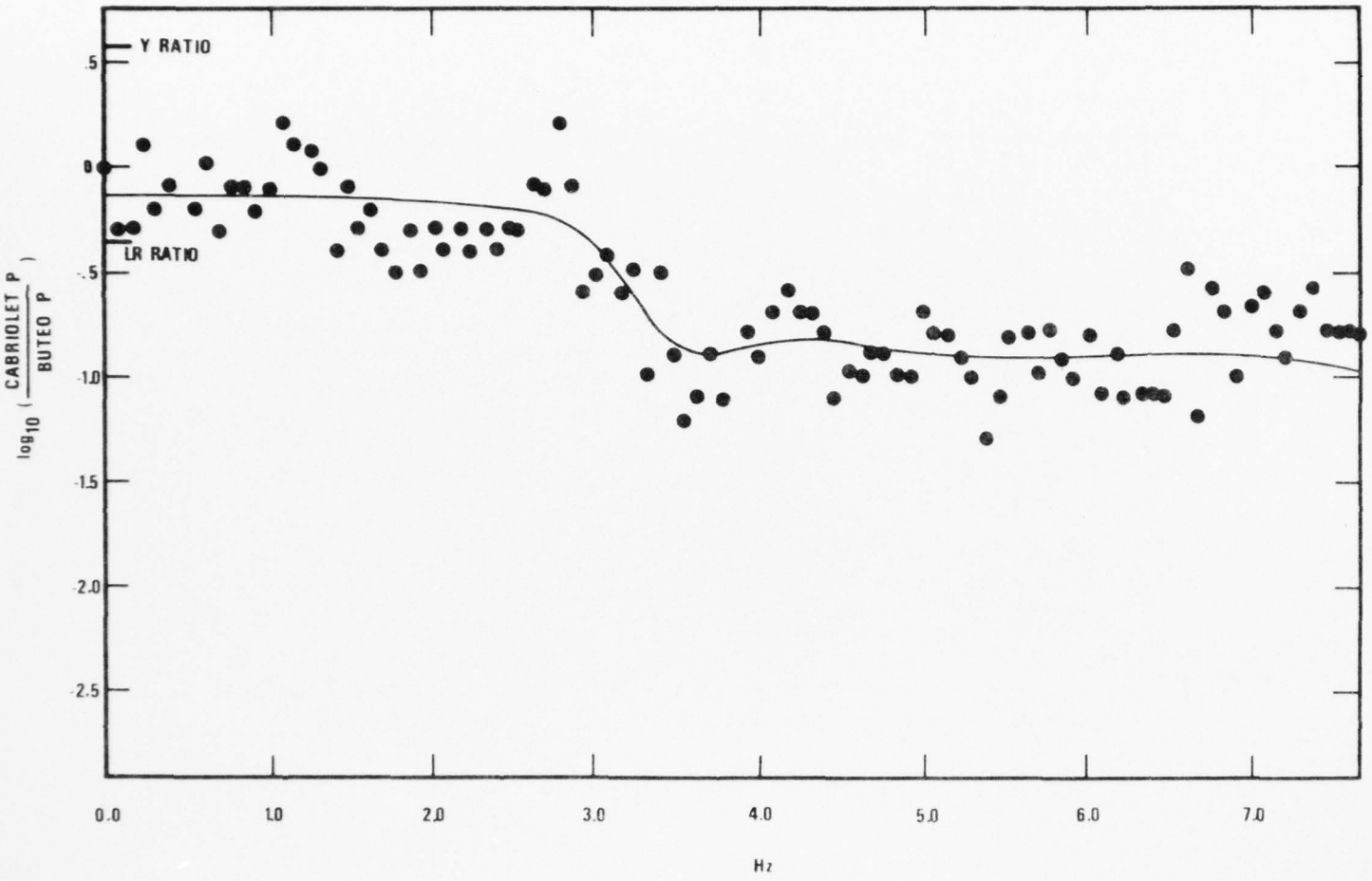

Figure 13f. Spectral ratios for cratering explosion: CABRIOLET/BUTEO.

Using $k_o = 10$, $B = 4$ as a match for the alluvium reduced potential in Haskell (1967), we were unable to find any pair of values k_o and B for SEDAN to obtain even a fair fit to the experimental data in Figure 13a.

The foregoing analysis failed to find a suitable well-defined scaling for SEDAN, SCHOONER, PALANQUIN, and CABRIOLET. This is, of course, the expected result since Haskell (1955), Sedov (1959) and Chabai (1965) have shown that for explosions in which the value of gravity (g) is an important parameter, cube-root scaling must fail in that the parameter c^2/gd (c is velocity of sound, d is a characteristic distance) must remain constant. To place this remark in context let us first develop the scaling theory, following Chabai (1965). Suppose we have:

Independent variables

a, radius of spherical explosive charge (L)

d, depth of burial of explosive charge (L)

p, a hydrostatic pressure ($ML^{-1}T^{-2}$)

W, mass of explosive charge (M)

E, energy of explosive charge (ML^2T^{-2})

R, distance from explosion center (L)

t, time after explosion (T)

Y, yield strength ($ML^{-1}T^{-2}$)

ν, viscosity ($ML^{-1}T^{-1}$)

Dependent variables

r, crater radius (L)

h, crater depth (L)

V, crater volume (L^3)

u, velocity of medium particle (LT^{-1})

Haskell, N. A., 1955, Some considerations on the modelling of crater phenomena in earth, Air Force Surv. Geophys. 67, TN-55-205, Air Force Cambridge Research Center, Bedford, Massachusetts.

Sedov, L. I., 1959, Similarity and Dimensional Methods in Mechanics, p. 256, Academic Press, New York and London.

α, acceleration of medium particle (LT^{-2})

σ, stress on medium particle ($ML^{-1}T^{-2}$)

τ, characteristic time, wave period (T)

Constant

g, gravity field strength (LT^{-2})

Other variables could also be included. Dimensionless quantities such as strain, void ratio, or moisture content of the medium can simply be inserted into the final result and will not affect the dimensional analysis of the listed variables. Quantities which have dimensions identical to those of variables listed--for example, heat capacity, or heat of vaporization c_v, explosive density ρ_x, detonation velocity D, or detonation pressure P--appear in the final result as the dimensionless ratios c_v/P, ρ_x/ρ, D/c, and P/p. Then the scaling relations when gravity is not important are:

$$r\left(\frac{\rho c^2}{E}\right)^{1/3} = H_1\left\{ d\left(\frac{\rho c^2}{E}\right)^{1/3} a\left(\frac{\rho c^2}{E}\right)^{1/3}, \frac{Y}{\rho c^2}, \frac{\nu}{(E\rho^2 c)^{1/3}}, \frac{p}{\rho c^2}, \frac{c_v}{\rho c^2} \right. \qquad (3)$$

$$\left. R\left(\frac{\rho c^2}{E}\right)^{1/3}, t\left(\frac{\rho c^5}{E}\right)^{1/3}, \ldots\ldots \right\}$$

$$h(\rho c^2/E)^{1/3} = H_2 \qquad (E/\rho c^8)^{1/3} = H_5$$

$$V(\rho c^2/E) = H_3 \qquad u/c = H_6$$

$$\sigma/\rho c^2 = H_4 \qquad \tau(\rho c^5/E)^{1/3} = H_7$$

And when gravity is important:

$$r\left(\frac{\rho c^2}{E}\right)^{1/3} = I_1\left\{ d\left(\frac{\rho c^2}{E}\right)^{1/3}, a\left(\frac{\rho c^2}{E}\right)^{1/3}, \frac{Y}{\rho c^2}, \frac{\nu}{(E\rho^2 c)^{1/3}}, \frac{p}{\rho c^2}, \frac{c_v}{\rho c^2}, \right. \qquad (4)$$

$$\left. R\left(\frac{\rho c^2}{E}\right)^{1/3}, t\left(\frac{\rho c^5}{E}\right)^{1/3}, \frac{c^2}{gd}, \ldots\ldots \right\}$$

$$h(\rho c^2/E)^{1/3} = I_2 \qquad (E/\rho c^8)^{1/3} = I_5$$

$$h(\rho c^2/E) = I_3 \qquad u/c = I_6$$

$$\sigma/\rho c^2 = I_4 \qquad r(\rho c^5/E)^{1/3} = I_7.$$

Equations (3) are the mathematical expression of "cube-root scaling". That is, assume constant values for p, ρ, c, Y, c_v, neglecting ν for the moment; then, if r, d, a, R, and t are proportional to $E^{1/3}$, equation 3 may be extended to other yields. Since $\nu/E^{1/3}$ would not be constant for ν = constant, we assume that viscosity is unimportant, or, to put it another way, that ν is large enough or small enough that its particular value has no influence on the solution. In the near-field this may well be the case since this region is dominated by shock waves in which it is well-known that if the viscosity is weak enough, the dissipation is independent of viscosity. Cherry et al (1975b), following Wilkins (1964), have only an "artificial" viscosity to maintain continuity across shocks. The particular value of the viscosity does not appreciably effect the final solution.

The far-field signal does depend on viscosity (Q) but in this case we feel that we have an adequate model of a linear dissipative system which enables us to cancel out the effects by spectral ratios. Thus we may scale the reduced displacement potential and combine it with mathematical operators which incorporate the parameter Q to examine the complete variation with yield.

It is of course true that gravity is important even in overburied explosions in that it contributes to the overburden pressure P_o. However, if that overburden pressure is constant, then the actual values of depth and gravity should be unimportant. (Depth of course influences pP and creates nulls in the spectrum independent of yield; these we take account of by physical models "tacked on" to the scaled source spectrum.) Examination

---

Wilkins, M. L., 1964, Calculations of Elastic-Plastic Flow, Methods in Computational Physics, 3, Academic Press.

of Figure 3.7 in Cherry et al. (1975b) together with the increase of pressure of 300 bars/km suggests that the effects on the signals of overburden pressure variation for the first five events in Table 1 will be on the order of 0.1 magnitude units.

The actual value of gravity will, however, clearly become important in the case of spall or cratering where, for example, the time spent in free fall is linearly related to the value for g.

The influence of gravity is seen in equations 4 in term c^2/gd which must be constant for similarity to hold. But if ρ and c^2 are constant, then d must scale as $E^{1/3}$. Since g cannot scale, we cannot attain similarity in a medium with constant properties.

If we insist that ρ and g remain constant but allow other material properties to vary, we may obtain the fourth-root scaling rule (Haskell, 1955; Sedov, 1959). Set

$$Y_1/Y_2 = p_1/p_2 = \rho_1 {c_1}^2/\rho_2 {c_2}^2 = \rho_1 g_1 d_1/\rho_2 g_2 d_2 = (\rho_1 g_1/\rho_2 g_2)^{3/4} (E_1/E_2)^{1/4},$$

$$v_1/v_2 = ({\rho_1}^5 g_1/{\rho_2}^5 g_2)^{1/8}(E_1/E_2)^{3/8},\ t_1/t_2 = (\rho_2 {g_2}^5/\rho_1 {g_1}^5)^{1/8} (E_1/E_2)^{1/8},$$

$$c_1/c_2 = (\rho_2 {g_1}^3/\rho_1 {g_2}^3)^{1/8} (E_1/E_2)^{1/8}, \qquad (5)$$

then:

$$r_1/r_2 = d_1/d_2 = R_1/R_2 = a_1/a_2 = (\rho_2 g_2/\rho_1 g_1)^{1/4} (E_1/E_2)^{1/4}, \qquad (6)$$

and the first of equations (4) may be rewritten in the more informative way:

$$r\left(\frac{\rho g}{E}\right)^{1/4} = I_1\left\{ d\left(\frac{\rho g}{E}\right)^{1/4},\ a\left(\frac{\rho g}{E}\right)^{1/4},\ \frac{Y}{(\rho^3 g^3 E)^{1/4}},\ \frac{Y}{(\rho^5 g E^3)^{1/8}},\right.$$

$$\left. \frac{p}{(\rho^3 g^3 E)^{1/4}},\ R\left(\frac{\rho g}{E}\right)^{1/4},\ t\left(\frac{\rho g^5}{E}\right)^{1/8},\ c\left(\frac{\rho}{g^3 E}\right)^{1/3},\ldots \right\} \qquad (4a')$$

From the above remarks we should not be surprised if we find it difficult to find a simple yield scaling for seismic data from cratering explosions. We might also remark that the overburden pressure varies markedly between these events, so that even if cube-root scaling were valid we would not be able to scale from the deeper events.

In Figure 14 we see the depth of the events considered in this report plotted as a function of their yields. We see how BUTEO and REX were vastly overburied, and how the depths for the events CABRIOLET, PALANQUIN, and SCHOONER follow neither cube-root or fourth-root scaling. Thus we are not surprised to see in Figure 15 how the long-period LR from the PAHUTE MESA cratering series fails to follow a slope of 1.0, as it would certainly do if it could be described by a single reduced displacement potential which could be scaled with yield. Evidently the basic 5 kt reduced displacement potential is greater for SCHOONER than for CABRIOLET or PALANQUIN. This might be due to more competent media properties, or to variation due to the c^2/gd parameter.

Note the excellent correlation of long-period LR amplitude with yield for the contained series. (Of course this is mostly an artifact since the yields of 0.7 and 19 kt for BUTEO and REX were determined by linear scaling from SCOTCH and BENHAM.) Note how this line is approximately 0.5 magnitude units above the DURYEA point.

The situation with respect to LR coupling for cratering and contained explosions is not clear; SCHOONER and DURYEA, both in tuff, have LR values in proportion to their yield although the depths are quite different; whereas SEDAN and PAR, in alluvium, show that the cratering explosion has a substantially greater LR. The explanation may be that the SEDAN/PAR proportion is correct and that DURYEA, being close to the water table has enhanced LR due to partial saturation. In dry tuff the LR would be lower.

Comparison of PAR in dry alluvium with the saturated tuff line shows a difference in coupling of 1.8 magnitude units. This compares to a difference of 1.3 magnitude units found by Marshall et al. (1971) citing Evernden and

---

Marshall, P. D., A. Douglas, and J. Hudson, 1971, Surface waves from underground explosions, Nature, v. 234, p. 8-9.

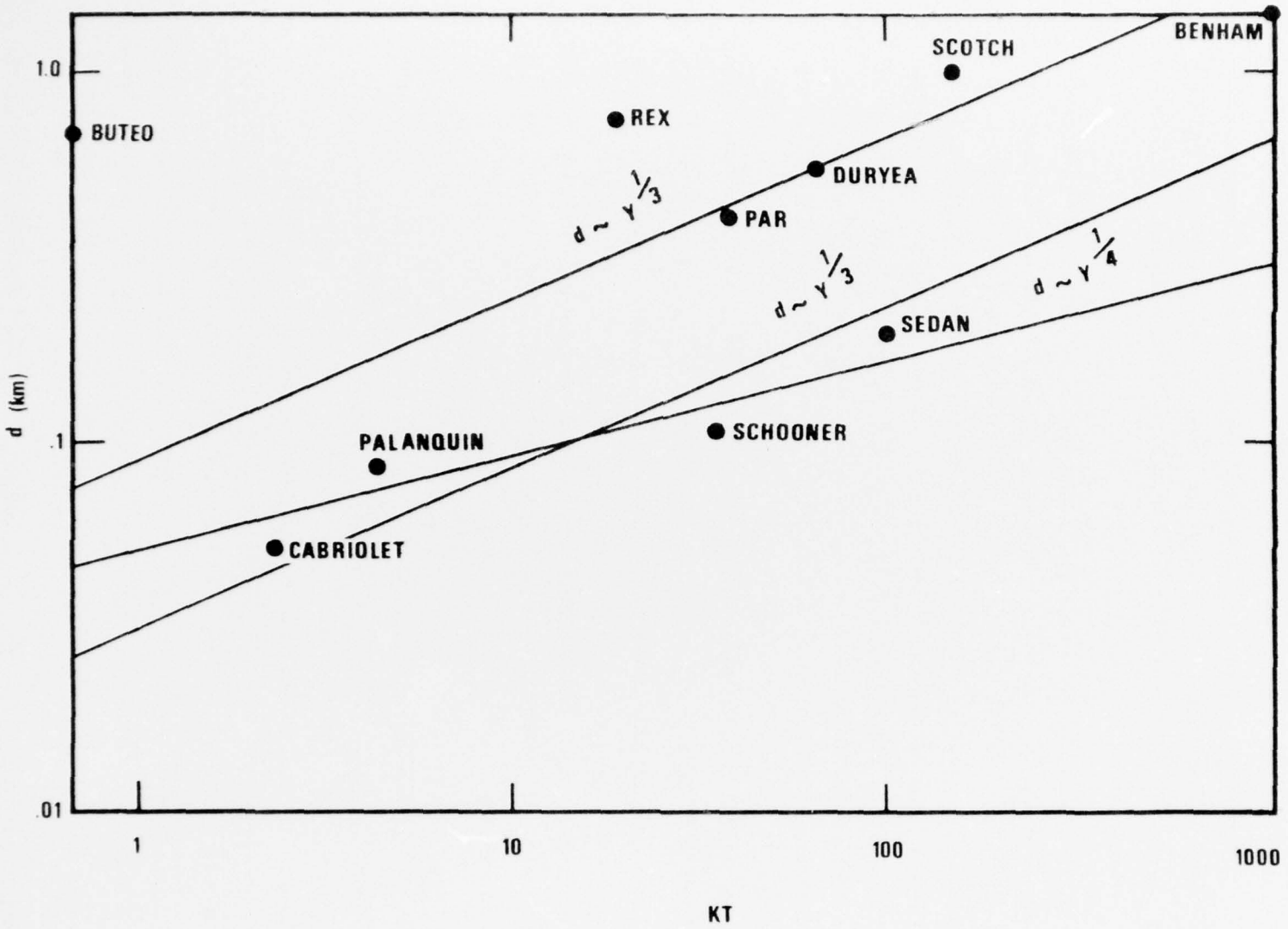

Figure 14. Depth of burial versus yield for the events considered in this study.

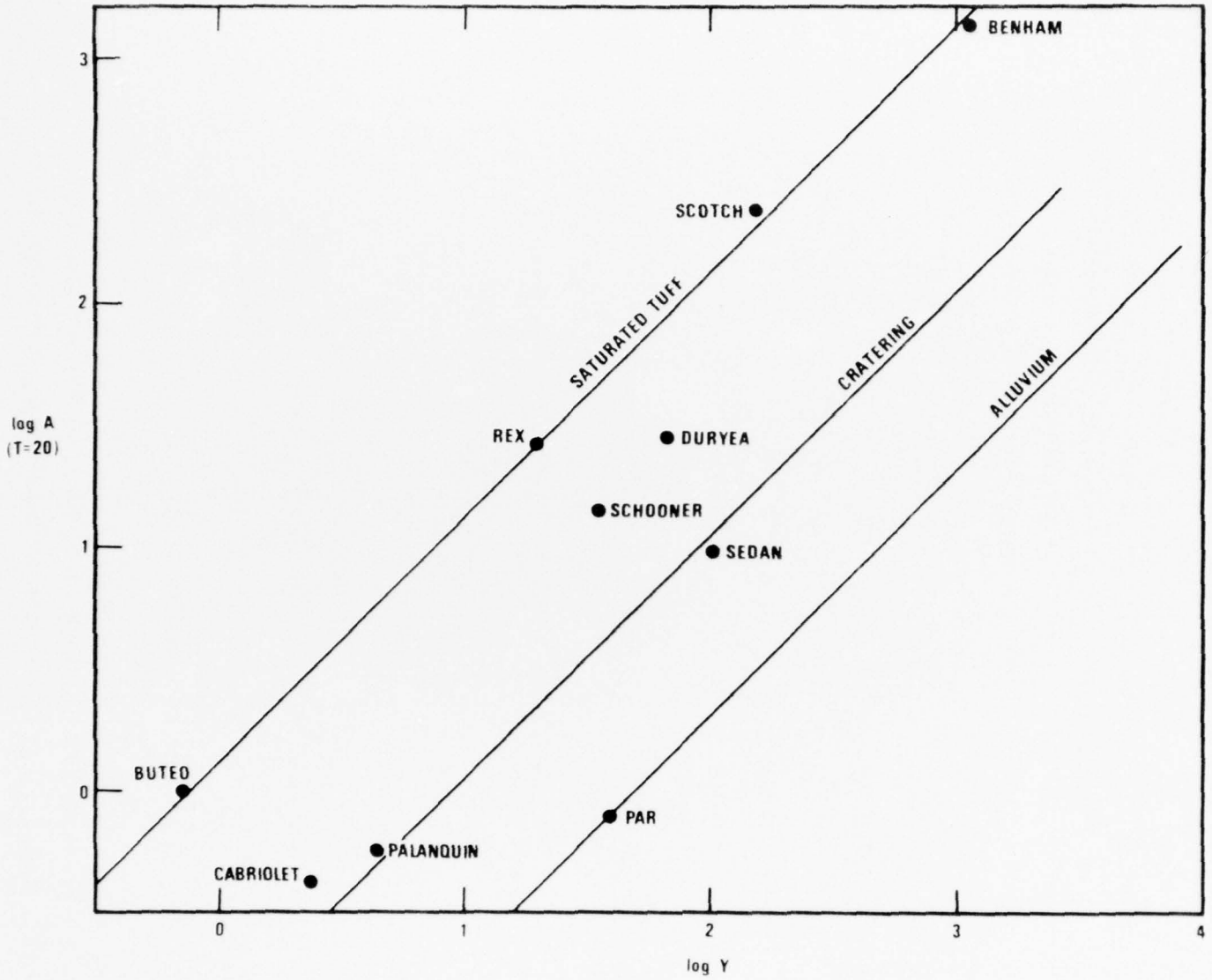

Figure 15. Relative amplitude of long-period LR radiation versus yield for events considered in this study. Yields of BUTEO and REX were estimated in this study by comparison of LR amplitudes with respect to BENHAM and SCOTCH, events with known yields.

Filson (1971) and Wagner (1970). However, considering that the alluvium shots have low amplitudes and are detected only at nearby stations; and that at these nearby stations the signals from larger events are apt to be distorted by non-linearities, we tend to prefer the relative amplitudes given in this report. Although the data are fewer by comparison to earlier studies, they have been measured in a manner designed to avoid these serious biasing effects.

Evernden, J. and J. Filson, 1971, Regional dependence of surface-wave versus body-wave magnitudes, J. of Geophys. Res., v. 75, p. 3303-3308.

Wagner, D., 1970, Nuclear yields from Rayleigh waves, Earthquake Notes, v. 16, p. 9-20.

CONCLUSIONS

In this study we have uncovered an apparent paradox. The RAINIER reduced displacement potential coupled with cube-root scaling gives a satisfactory explanation of the relative Rayleigh and body-wave spectra as observed at KNUT and MNNV. However, the same potentials cannot explain the observed amplitude-yield relations at teleseismic distances. The only apparent way out of this paradox is to assume that the source is asymmetric and that the signals departing vertically downward to teleseismic distances are different from those departing more nearly horizontally which are used to determine the reduced displacement potential and which travel to nearby seismic stations.

The most unambiguous way to settle this question would be to measure the reduced displacement potential simultaneously above, below, and to the side of a suitable underground test. A less satisfactory approach would be a finite difference 2-dimensional calculation which will give the RAINIER measurements or measurements from another shot in tuff at the side and vertically above; then one would see what displacement the same computer run gives for directly below the test. Differences of some degree must be expected for we know that spalling occurs near the surface, and that the shattered zone resulting from an explosion extends upward farther than downward. Note that asymmetry in the source calls into question the entire concept of a reduced displacement potential whose existence is derived in the context of spherical symmetry.

The fact that scaling is so difficult for cratering explosions suggests either that model experiments will have to be carried out or that finite difference calculations will have to be performed in order to predict results from future cratering explosions. The results reported in this study could serve as useful calibration points for these approaches.

REFERENCES

Blandford, R. and D. Clark, 1974, Detection of long-period S from earthquakes and explosions at LASA and LRSM stations with application to positive and negative discrimination of earthquakes and underground explosions, SDAC-TR-74-15, Teledyne Geotech, Alexandria, Virginia. ADA 013 672.

Blandford, R., 1975, A source theory for complex earthquakes, Bull. Seism. Soc. Am., v. 65, p. 1385-1406.

Bridgman, P. W., 1949, Dimensional Analysis, Yale University Press, New Haven, Connecticut.

Carpenter, E. W., R. A. Savill, and J. K. Wright, 1962, The dependence of seismic signal amplitudes on the size of underground explosions, Geophysical Journal, v. 6, p. 426-440.

Carpenter, E. W., 1966, A quantitative evaluation of teleseismic explosion records, Proc. Roy. Soc., A., v. 290, p. 396-407.

Chabai, A. J., 1965, On scaling dimensions of craters produced by buried explosions, J. Geophys. Res., v. 70, p. 5075-5098.

Cherry, J. T., N. Rimer, J. M. Savino, and W. O. Wray, 1975a, Improved yield determination and event identification research, SSS-R-75-2696, Systems, Science, and Software, LaJolla, California.

Cherry, J. T., N. Rimer, and W. O. Wray, 1975b, Seismic coupling from a nuclear explosion: the dependence of the reduced displacement potential on the non-linear behavior of the near-source rock environment, SSS-T-76-2742, Systems, Science and Software, LaJolla, California.

Cohen, T. J., R. L. Sax, and H. L. Husted, 1972, Spectral whitening with application to explosion pP, Seismic Data Laboratory Report 282, Teledyne Geotech, Alexandria, Virginia. AD 750 781.

Der, Z. A. and T. W. McElfresh, 1975, Short-period P-wave attenuation along various paths in North America as determined from P-wave spectra of the SALMON nuclear explosion, SDAC-TR-75-16, Teledyne Geotech, Alexandria, Virginia.

REFERENCES (Continued)

Douglas, A., J. A. Hudson, and C. Blamey, 1972, A quantitative evaluation of seismic signals at teleseismic distances--III computed P and Rayleigh wave seismograms, Geo. J. R. Astr. Soc., v. 28, p. 385-410.

Evernden, J. R., 1970, Magnitude versus yield of explosions, J. Geophys. Res., v. 75, p. 1028-1032.

Evernden, J. and J. Filson, 1971, Regional dependence on surface-wave versus body-wave magnitudes, J. Geophys. Res., v. 75, p. 3303-3308.

Frasier, C. W., 1972, Observations of pP in the short-period phases of NTS explosions recorded at Norway, Geophys. J. R. Astr. Soc., v. 31, p. 99-109.

Frasier, C. W. and J. R. Filson, 1972, A direct measurement of the earth's short-period attenuation along a teleseismic ray path, J. Geophys. Res., v. 77, p. 3782-3787.

Glover, P. and S. S. Alexander, 1970, A comparison of the Lake Superior and Nevada Test Site source regions, Seismic Data Laboratory Report 243, Teledyne Geotech, Alexandria, Virginia. AD 865 512

Haskell, N. A., 1955, Some considerations on the modelling of crater phenomena in earth, Air Force Surf. Geophys. 67, TN-55-205, Air Force Cambridge Research Center, Bedford, Massachusetts.

Haskell, N. A., 1967, Analytic approximation for the elastic radiation from a contained underground explosion, J. Geophys. Res., v. 72, p. 2583-2587.

Latter, A. L., E. A. Martinelli, and E. Teller, 1959, Seismic scaling law for underground explosions, Physics of Fluids, v. 2, p. 280-282.

Lyuke, E. I., S. K. Datagan, and V. E. Peregontseva, 1976, Forecasting the Seismic wave spectra of large underground detonations from the spectra of small preliminary explosions, Izvestia, Physics of the Solid Earth, v. 12, p. 103-109.

Marshall, P. D., A. Douglas, and J. Hudson, 1971, Surface waves from underground explosions, Nature, v. 234, p. 8-9.

Marshall, P., 1972, Some seismic results from a world-wide sample of large underground explosions, AWRE O 49/72, Aldermaston, Berkshire.

REFERENCES (Continued)

Mueller, R. A. and J. R. Murphy, 1971, Seismic characteristics of underground nuclear detonations: Part I, Seismic scaling law of underground detonations, Bull. Seism. Soc. Am., v. 61, p. 1675-1692.

Noponen, I., 1975, Compressional wave power spectrum from seismic sources, Institute of Seismology, University of Helsinki, ISBN 951-45-0538-7. Contract AFOSR-72-2377 Final Report.

Peppin, W. A., 1974, Discrimination among small magnitude events on Nevada Test Site, Geophys. J. R. Astr. Soc., v. 37, p. 227-243.

Rodean, H. C., 1972, Nuclear-Explosion Seismology, U. S. Atomic Energy Commission, Division of Technical Information.

Sacks, I., 1966, A broad-band large dynamic range seismograph, The Earth Beneath the Continents, p. 543-554, ed. J. Steinhard, American Geophysical.

Sedov, L. I., 1959, Similarity and Dimensional Methods in Mechanics, p. 256, Academic Press, New York and London.

Springer, D. L., 1966, P-wave coupling of underground nuclear explosions, Bull. Seism. Soc. Am., v. 56, p. 861-876.

Springer, D. L. and R. L. Kinnaman, 1971, Seismic source summary for U. S. underground nuclear explosions, 1961-1970, v. 61, p. 1073-1098.

Springer, D. and W. Hannon, 1973, Amplitude-yield scaling for underground nuclear explosions, Bull. Seism. Soc. Am., v. 63, p. 477-500.

Toksöz, M. N. and H. H. Kehrer, 1972, Tectonic strain release by underground nuclear explosions and its effect on seismic discrimination, Geophys. J. R. Astr. Soc., v. 31, p. 141-161.

Trembly, L. D. and J. W. Berg, 1968, Seismic source characteristics from explosion-generated P waves, Bull. Seism. Soc. Am., v. 58, p. 1833-1848.

von Seggern, D. H., 1973, Joint magnitude determination and analysis of variance for explosion magnitude estimates, Bull. Seis. Soc., Am., v. 63, #3, p. 827-845.

von Seggern, D. H. and R. Blandford, 1972, Source time functions and spectra for underground nuclear explosions, Geophys. J. R. Astr. Soc., v. 31, p. 83-97.

von Seggern, D. H. and D. G. Lambert, 1972, Analysis of teleseismic data for the nuclear explosion MILROW, Seismic Data Laboratory Report 258, Teledyne Geotech, Alexandria, Virginia. AD 743 072.

Wagner, D., 1970, Nuclear yields from Rayleigh waves, Earthquake Notes, v. 16, p. 9-20.

Werth, G. C., R. F. Herbst, and D. L. Springer, 1962, Amplitudes of seismic arrivals from the M discontinuity, J. Geophys. Res., v. 67, p. 1587-1610.

Wilkins, M. L., 1964, Calculations of Elastic-Plastic Flow, Methods in Computational Physics, 3, Academic Press.